frontiers | Frontiers in Immunology

TYPE Original Research
PUBLISHED 12 December 2025
DOI 10.3389/fimmu.2025.1644433

OPEN ACCESS

EDITED BY
Won Fen Wong,
University of Malaya, Malaysia

REVIEWED BY
Yunliang Yao,
Huzhou University, China
Mohan Das,
Indian Institute of Technology Kharagpur, India

*CORRESPONDENCE
Fangyu Wang
wangfy65@yeah.net

†These authors have contributed equally to this work

RECEIVED 10 June 2025
REVISED 21 November 2025
ACCEPTED 25 November 2025
PUBLISHED 12 December 2025

CITATION
Shi S, Tang G, Wei J, Shen S, Ding Z, An Q, Tao H and Wang F (2025) Organosilicone double-long-chain diquaternary ammonium salt acts as a biofilm scavenger to ameliorate colitis induced by dextran sulfate sodium salt. *Front. Immunol.* 16:1644433. doi: 10.3389/fimmu.2025.1644433

Organosilicone double-long-chain diquaternary ammonium salt acts as a biofilm scavenger to ameliorate colitis induced by dextran sulfate sodium salt

Shaopei Shi[1†], Guoxing Tang[2†], Juan Wei[2], Si Shen[2], Zhihao Ding[2], Qin An[2], Hui Tao[2] and Fangyu Wang[2*]

[1]Department of Nephrology, Jiangning Hospital Affiliated to Nanjing Medical University, Nanjing, Jiangsu, China, [2]Department of Gastroenterology, Jinling Hospital of Nanjing Medical University/ General Hospital of Eastern Theater Command, Nanjing, Jiangsu, China

Objective: The treatment of ulcerative colitis (UC) remains challenging due to limited efficacy and significant side effects. Organosilicone Double-Long-Chain Diquaternary Ammonium Salt (JUC Spray Dressing) exhibits antibacterial, anti-inflammatory, and wound-healing properties. This study aimed to evaluate the therapeutic effects of JUC Spray Dressing in a Dextran Sulfate Sodium Salt (DSS)-induced UC mouse model and explore its potential mechanisms of action.

Methods: A UC model was induced in mice using 3% DSS, followed by JUC Spray Dressing enema treatment. Disease activity index (DAI), histological scores, bacterial biofilms on the intestinal mucosa, and tight junction integrity were assessed. Inflammatory cytokine levels in peripheral blood were measured, and 16S rDNA amplicon sequencing was performed to analyze cecal microbiota composition.

Results: JUC Spray Dressing significantly alleviated UC symptoms and reduced colonic congestion, with no significant difference compared to other treatment groups ($P > 0.05$). All treatments significantly decreased the expression of inflammatory cytokines in peripheral blood ($P < 0.0001$), with no significant differences among the groups. Additionally, all treatments effectively reduced biofilm thickness and bacterial abundance, improving intestinal barrier integrity. JUC Spray Dressing inhibited harmful bacteria such as *Bacteroides* spp. without significantly altering overall microbial composition.

Conclusions: JUC Spray Dressing effectively removes intestinal bacterial biofilms, reduces inflammation, and enhances barrier function to alleviate UC symptoms. Its efficacy appeared comparable to conventional treatments, suggesting potential as an alternative therapeutic option; however, the present study did not assess mucosal safety, and dedicated toxicology studies are required to establish safety for intraluminal use.

KEYWORDS

ulcerative colitis, bacterial biofilm, organosilicone double-long-chaindiquaternary ammonium salt, treatment, colitis

1 Introduction

Inflammatory bowel disease (IBD) is a chronic inflammatory condition of the gastrointestinal tract that encompasses Crohn's disease (CD) and ulcerative colitis (UC) (1). With rapid industrialization and the increasing westernization of dietary habits in China, the incidence of IBD has been rising annually, making it a prevalent digestive disorder (2). Although the exact pathogenesis of IBD remains unclear, it is believed to involve multiple factors, including genetic predisposition, intestinal barrier dysfunction, and gut microbiota imbalances (3–5). Most patients with IBD suffer from recurrent episodes with incomplete remission. Bacterial biofilms are strongly implicated in the pathogenesis of IBD (6). When bacteria adhere to biotic or abiotic surfaces, they secrete proteins and mucopolysaccharides that facilitate biofilm formation, creating structured microbial communities. Once mature, biofilms release bacterial cells that disseminate to new sites, leading to the formation of additional biofilms and perpetuating chronic infection. Bacteria within biofilms are embedded in an extracellular polymeric substances (EPS) matrix, which serves as a protective barrier, enhancing bacterial resistance to external stressors (7). In patients with IBD, the intestinal barrier is compromised, allowing bacteria to penetrate the mucus layer and directly interact with the intestinal epithelium, thereby promoting biofilm formation and exacerbating inflammation. As such, bacterial biofilms in the intestinal mucosa are detected at higher rates in patients with IBD.

Current treatment options for IBD, including 5-aminosalicylic acid (5-ASA, mesalazine), glucocorticoids, immunosuppressants, and biologic agents, are limited by severe adverse effects and high costs. Consequently, the development of novel therapeutic strategies is urgently needed (8). 5-ASA is an anti-inflammatory drug with a chemical structure similar to that of acetylsalicylic acid. The exact mechanism of 5-ASA against UC is unclear; however, 5-ASA reportedly inhibits the production of prostaglandins and leukotrienes, resulting in anti-inflammatory effects. In addition, 5-ASA can inhibit nuclear factor-kB (NF-κB), regulate PPAR-γ receptors, and inhibit DNA damage to the intestinal mucosa mediated by reactive oxygen species (9).

Oral antibiotics can also improve the course of refractory UC. Antibiotics, such as amoxicillin, metronidazole (MTZ), and ciprofloxacin, are commonly used as adjuvant treatments for IBD. In a randomized multi-center trial in Japan, patients with UC who received combined antibiotic treatment achieved more effective clinical remission and endoscopic healing (10). However, the use of antibiotics upsets the balance between bacteria and fungi in the intestine. Fungi, particularly *Candida albicans*, have a potentially pathogenic effect as a precipitating factor for IBD (11). In addition, the use of broad-spectrum antimicrobials increases the probability of *Clostridium difficile* infection in patients with active disease, which is the most common infectious complication in patients with IBD, and further increases the risk of colectomy (12). Therefore, the identification of therapeutic alternatives to antibiotics is a key research goal.

Several studies have shown that targeted regulation of intestinal bacterial biofilms can alleviate experimental colitis in mice (13, 14). Quaternary ammonium salt (QAS) is a cationic ammonium salt formed when the four hydrogen ions of the ammonium ions are substituted by hydrocarbon groups. QAS is a common germicidal component that is adsorbed on the surface of the thallus, with the hydrophobic group inserted into the lipid layer, which permeabilizes and destroys the cell membrane, eventually disrupting cell metabolism and leading to the death of the fungus. In addition, QAS interferes with the synthesis of nucleic acids and proteins (15). Therefore, we hypothesized that QAS could relieve UC by clearing intestinal bacterial biofilms. JUC Spray Dressing (name of U.S. FDA and CE certifications, while the medical device name in China is Long-acting Antimicrobial Material) is a new Organosilicone Double-Long-Chain Diquaternary Ammonium Salt formulation that benefits from the high hydrophobicity of silicone, which further improves the water solubility of the compound. When JUC Spray Dressing contacts the skin or mucosal surfaces, it forms a double antibacterial layer, including an adhesive layer and a positively charged layer. The adhesive layer ensures that the salt can stick to the surface, while the positive cations interact with the negatively charged cell wall and membrane via electrostatic forces in a destructive manner, resulting in bactericidal effects. A previous study has shown that JUC Spray Dressing can prevent bacterial growth by physically killing various bacteria (16). The product is now widely used in wound treatment and indwelling care. Although JUC Spray Dressing has been proven to be safe and non-toxic for humans, information is lacking regarding its bactericidal effects on intestinal bacteria (17).

Therefore, this study aimed to evaluate the therapeutic effects of JUC Spray Dressing in a DSS-induced mouse model of UC. Additionally, we explored its mechanisms of action by analyzing biofilms via electron microscopy, assessing intestinal barrier function, and examining microbial community dynamics.

Given that ulcerative colitis involves mucosal biofilm formation, we selected a colonic topical delivery model to test a biofilm-targeting agent (JUC Spray Dressing). This approach was intended to maximize local biofilm removal at the disease site while limiting systemic exposure. Nevertheless, gastrointestinal mucosal pharmacokinetics and intraluminal retention of JUC in this setting have not yet been defined and will require dedicated studies.

Abbreviations: IBD, Inflammatory bowel disease; UC, ulcerative colitis; CD, Crohn's disease; EPS, extracellular polymeric substances; 5-ASA, 5-aminosalicylic acid; NF-kB, nuclear factor-kB; MTZ,metronidazole; QAS, Quaternary ammonium salt; DSS, Dextran Sulfate Sodium Salt; DAI, disease activity index; SEM, scanning electron microscope; TEM, transmission electron microscope; NSAIDs, non-steroidal anti-inflammatory drugs.

2 Methods

2.1 Reagents

DSS (molecular weight: 36,000–50,000 Da) was obtained from MP Biomedicals (Santa Ana, CA, USA). The fecal occult blood

detection kit was purchased from the Jiancheng Institute of Biological Engineering (Nanjing, China). Mouse enzyme-linked immunosorbent assay (ELISA) kits for interleukin-6 (IL-6), interleukin-1β (IL-1β), and tumor necrosis factor-alpha (TNF-α) were obtained from R&D Systems (Minneapolis, MN, USA). Chloral hydrate solution was sourced from Legend Biotech (Beijing, China). MTZ (0.5 g/100 mL) was provided by Shijiazhuang Siyao Co. Ltd. (Shijiazhuang, China), and mesalazine (28 g/60 mL) was obtained from Dr. Falk Pharma GmbH (Freiburg im Breisgau, Germany). JUC Spray Dressing was purchased from NMS Technologies Co., Ltd. (Nanjing, China).

2.2 Animal experimental design

A small sample size was chosen as this study represents the first *in vivo* evaluation of JUC Spray Dressing, with the primary objective of obtaining preliminary data for subsequent, more complex experimental studies. Male C57BL/6J mice (6–8 weeks old, 20–24 g, n=50) were purchased from Charles River (Zhejiang, China) and housed under constant conditions (20 ± 2 °C, humidity 45 ± 5%, 12-hour light/dark cycle, five mice per cage) with standard rat feed available ad libitum. After acclimation for one week, the mice were randomly divided into five groups (n=10) as follows: normal control group, DSS plus phosphate-buffered saline (DSS+PBS) group, DSS plus JUC Spray Dressing (DSS+JUC) group, DSS plus metronidazole (DSS+MTZ) group, and DSS plus mesalazine (DSS + 5-ASA) group. The 10 mice per treatment group were reared in two cages. Mice were randomly assigned to groups using the RAND() function in Microsoft Excel 2021. The UC mouse model was established with DSS according to a previously described method (18). Briefly, mice were administered fresh 3%(w/v) DSS freely for seven consecutive days, resulting in acute UC. Mice in the normal control group were free to drink sterile water. On day 7, mice received enemas (200 μM/mouse, 0.008 mL/g/day) containing PBS, JUC, MTZ (1 g/L), or 5-ASA every other day (19, 20). Prior to enema administration, mice were fasted for 12 hours and anesthetized via intraperitoneal injection of 10% (v/v) chloral hydrate (50 μM/mouse), which took effect within 5–10 minutes. Enema administrations were performed between 12:30 and 14:30 on each treatment day, and the order of group treatments was randomized to minimize circadian or operator bias. All procedures were standardized across groups to ensure consistency. After the enema, each mouse was suspended by its tail upside down for 2 minutes and then returned to its original cage. During the experiment, changes in body weight, occult blood, diarrhea, and stool consistency were observed and recorded daily and the disease activity was scored. The test was performed between 12.30 pm and 2.30 pm and the testing order was randomized daily,with each animal tested at a different time on each test day. The minimum allowed mouse weight before euthanasia was 15 g. At the end of the experiment (day 12), the mice were euthanized, and the colon tissue 1 cm from the anus was excised and fixed with 4%(w/v) paraformaldehyde for subsequent experiments. Mice were anesthetized via intraperitoneal injection of chloral hydrate at 350 mg/kg. This regimen provides approximately 2 hours of anesthesia with relatively shallow depth and limited muscle relaxation; at high doses, myocardial contractility may be depressed and arrhythmias can occur, so animals were continuously monitored. No procedure-related perforation or premature death occurred. The remaining colon tissue was stored at −80°C. Each animal was evaluated by three different investigators, two of whom were blinded to the treatment group. Animals were included in the study if they underwent successful enema treatment or excluded if insertion of the enema resulted in perforation or if the animal died prematurely, thus preventing the collection of behavioral and histological data. All assessments were performed in a blinded fashion by three independent experimenters; inter−rater reliability was high ($\kappa > 0.8$), and discrepancies were resolved by consensus. No mice experienced perforation or premature death related to enema administration in this study; therefore, no animals were excluded due to procedural complications.

2.3 Assessment of inflammation

Changes in body weight, DAI, colon length, and histological score were used to evaluate the successful establishment of the UC mouse model and treatment effectiveness. All collected data were included in the analysis. The DAI was calculated as follows: 1) change in weight (0: <1%, 1: 1–5%, 2: 5–10%, 4: >15%), 2) stool consistency (0: normal, 2: loose, 4: diarrhea), and presence of blood in stool (0: negative, 2: positive, 4: gross bleeding). Colon tissue fixed with 4% (w/v) paraformaldehyde was embedded in paraffin, sectioned, and stained with hematoxylin and eosin. The histological conditions were then determined under light microscopy and scored based on crypt damage, ulceration, and neutrophil infiltration. The inflammation score was determined as follows:1) severity of inflammation (0: none; 1: slight; 2: moderate; 3: severe); 2) extent of inflammation (0: none; 1: mucosa; 2: mucosa and submucosa; 3: transmural); 3) extent of damage to the crypt (0: none; 1: basal 1/3 damage; 2: basal 2/3 damage; 3: only the surface epithelium intact; 4: entire crypt and epithelium lost); and 4) percentage of area infiltrated (1: 1–25%; 2: 25–50%; 3: 51–75%; 4: 76–100%). More than three high-power fields (×400) were randomly selected from each tissue section, and scores were assigned by two blinded independent researchers, with the average value taken as the result.

2.4 Immunohistochemistry and immunofluorescence

The expression of inflammatory cytokines in the colon was evaluated via immunohistochemical analysis. Endogenous peroxidase activity was inhibited, and tissue sections were incubated with a nonspecific staining blocking reagent. Next, sections were incubated with corresponding primary antibodies and HRP-conjugated secondary antibodies. Images of the slides were obtained using an Nikon E100 optical microscope (Nikon, Tokyo, Japan). A minimum of three fields per sample were randomly selected for imaging under a 40× objective lens, and

semi-quantitative protein expression analysis was conducted using ImageJ software. Protein expression intensity was expressed as the area occupied by the positive signal. The expression of tight junction (TJ)-associated proteins in the colon was evaluated using immunofluorescence. Images of the slides were obtained using an ECLIPSE TI-SR fluorescence microscope (Nikon). For IHC, staining was quantified using H–score/average optical density; for immunofluorescence (MUC2, ZO–1, occludin), mean fluorescence intensity was measured. Negative controls (omission of primary antibody) and isotype controls were included to verify staining specificity.

2.5 Measurement of goblet cells

After dewaxing and hydration, the paraffinized sections of colon tissue were immersed in distilled water, then dipped in periodic acid solution, maintained at room temperature for 1.5 hours, immersed in distilled water, dipped in Schiff's reagent, dewatered in an oven at 37 °C for 20 minutes, rinsed with distilled water for 10 minutes, dehydrated step-by-step, made transparent with xylene, and lastly sealed with neutral gum. Goblet cells in the colon stained dark blue, while the surrounding tissue appeared light blue or colorless. Image-pro Plus 6.0 software was used to analyze the sections.

2.6 Electron microscopy

The intestinal mucosa of three randomly selected mice in each group was observed by electron microscopy. Colon tissue 1 cm from the anus was fixed using 2.5% glutaraldehyde. Three microscopic fields were examined for each specimen. Biofilms on the intestinal mucosa were examined using an SU8100 scanning electron microscope (SEM; Hitachi, Tokyo, Japan), while tight junctions between epithelial cells were assessed using an HT7700 transmission electron microscope (TEM; Hitachi).

2.7 Serum cytokine analysis using ELISA

Serum was assayed for pro-inflammatory cytokines using specific ELISA kits (R&D Systems, Minneapolis, MN, USA) according to the manufacturer's instructions.

2.8 Sequencing analysis of 16S RNA amplicon

Genomic DNA was extracted from the mouse cecal contents using a Mag Pure Soil DNA KF Kit (Angen Biotech, Guangzhou, China), and DNA purity and concentration were detected by agarose gel electrophoresis. Using diluted genomic DNA as a template, polymerase chain reaction amplification and purification were performed using primers for the bacterial 16S rDNA (V3-V4) region (343-5'-TACGGRAGGCAGCAG-3': forward primer, 798R-5'-AGGGTATCTAATCCT-3': reverse primer). Based on sequence alignment, PyNAST software was used to construct the phylogenetic relationship of representative sequences of operational taxonomic units (OTUs). After pre-processing the sequencing data to generate high-quality sequences, the sequences were grouped into multiple OTUs according to their similarity. Finally, the alpha diversity, beta diversity, taxonomy, and flora composition of the microflora were analyzed and 16S functional gene prediction was performed.

2.9 Statistical analysis

GraphPad Prism software (GraphPad Software, La Jolla, CA, USA) was used to perform the statistical analysis and graph generation. The Kolmogorov–Smirnov method was used to analyze the data, and $P>0.1$ was considered indicative of normal distribution. One-way ANOVA was used to compare mean mouse body weight, colon length, and inflammatory factor levels among groups, followed by Tukey's *post hoc* test for pairwise comparisons. $P<0.05$ was considered to be a statistically significant difference.

3 Results

3.1 JUC Spray Dressing ameliorates colitis induced by DSS

During DSS-induced colitis, mice progressively developed symptoms including weight loss, diarrhea, and hematochezia (bloody stools). Compared to the normal control group, mice in the DSS+PBS group exhibited significantly reduced body weights and increased DAI scores. Following enema treatments, weight loss symptoms improved, and DAI scores significantly decreased ($P < 0.01$) in all three drug-treated groups. However, no statistically significant differences were observed among these groups ($P > 0.05$) (Figures 1A, B). These results demonstrated that JUC Spray Dressing could alleviate the symptoms of weight loss and decrease activity in mice with UC. Moreover, this effect was comparable to that achieved by MTZ or 5-ASA.

For the time-course endpoints shown in Figures 1A, B, the DSS +JUC group did not differ significantly from the DSS+PBS group ($p>0.05$). Between-treatment differences (JUC vs MTZ vs 5-ASA) likewise did not reach statistical significance.

Mice in the DSS+PBS group showed significant colonic contractures and their intestinal contents were unformed. The experimental results are shown in Figures 1C, D. Compared with those in the normal control group, colons in the DSS+PBS group were swollen and hyperemic, and the contractures were shortened ($P<0.0001$). Colon lengths in the DSS+JUC group were significantly increased ($P<0.05$) compared to those in the DSS+PBS group. All three drugs were effective in alleviating colon contracture in UC model mice.

Histopathology is an important source of information regarding colon health. As shown in Figures 1E, F, the colonic mucosa of the

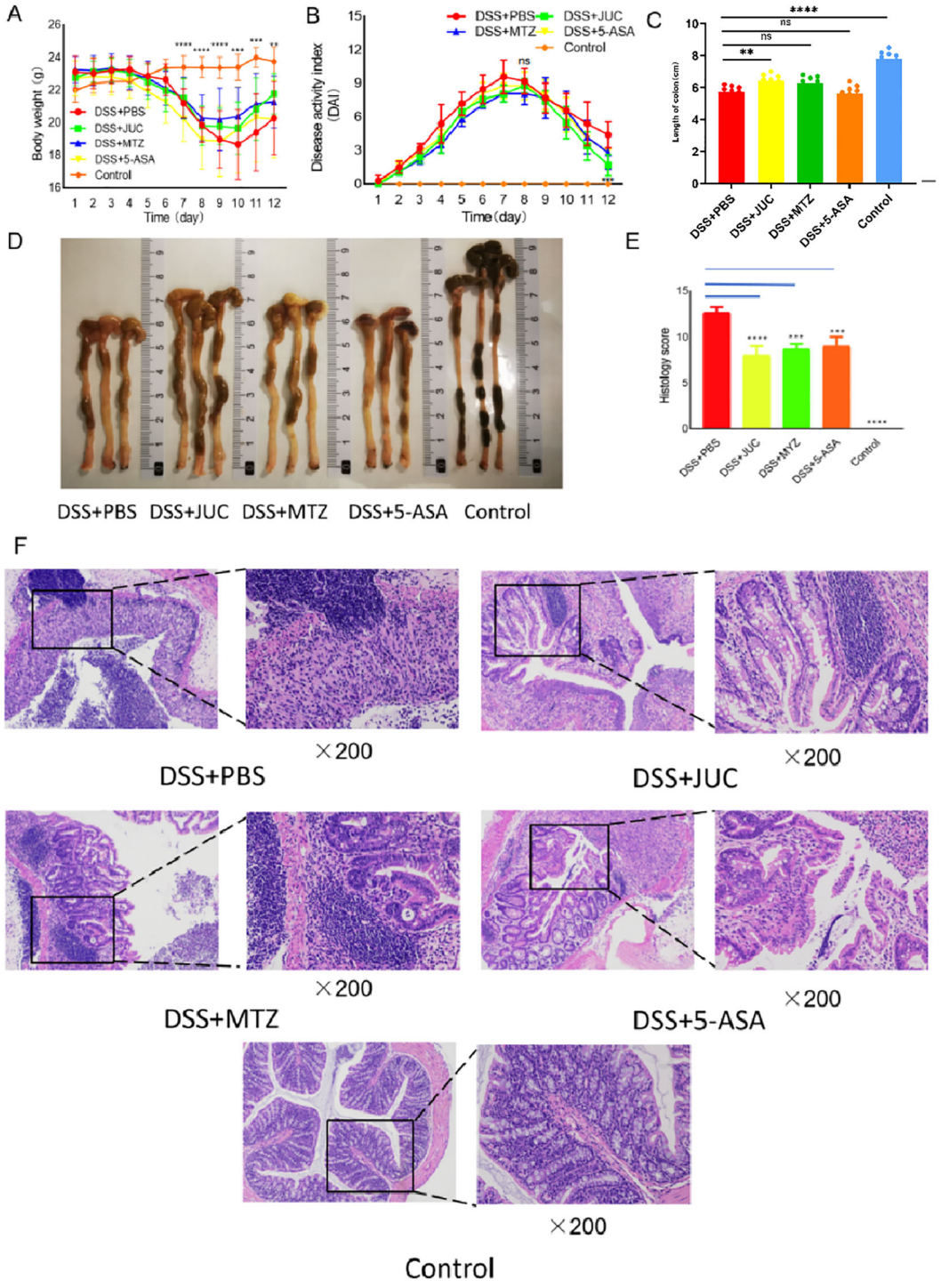

FIGURE 1
Effects of JUC Spray Dressing on intestinal inflammation in mice. **(A)** Changes in the body weights of mice (N = 10),**P<0.01,***P<0.001, ****P<0.0001,compared to the DSS+PBS group. **(B)** Changes in DAI scores (N = 10),***P<0.001,compared to the DSS+PBS group. **(C)** Comparison of colonic lengths between groups (N = 10), *P<0.05,****P<0.0001,compared to the DSS+PBS group. **(D)** Macroscopic view of a mouse colon. **(E)** Histological scores of mouse colon tissues,***P<0.001,****P<0.0001, compared to the DSS+PBS group. **(F)** Effects of drugs on colonic pathological changes in mice(HE,200×). Statistical analysis. Continuous multi-group comparisons (e.g., mouse body weight, panel 1A; colon length, panel 1C): Tukey's Honestly Significant Difference (HSD) test was used for multiple-comparison correction to rigorously evaluate pairwise differences in group means. Ordinal/score outcomes (e.g., disease activity index, panel 1B; histopathology score, panel 1E): Student's t-test was applied if the data approximately met normality and homoscedasticity assumptions; otherwise, the non-parametric Mann–Whitney U test was used. A two-sided $P < 0.05$ was considered statistically significant.

normal control group was intact, the glands were neatly arranged, and no inflammatory edema was observed. In the DSS+PBS group, colon tissue damage was severe, the intestinal mucosa exhibited shedding and necrosis, typical crypt abscess formation was observed, along with glandular deletion, partial crypt damage, and fewer goblet cells, and extensive infiltration of inflammatory cells and transmural inflammation occurred. JUC Spray Dressing, MTZ, and 5-ASA enema therapy alleviated inflammatory cell infiltration and reduced the depth and extent of lesions, thereby reducing the histological score ($P<0.001$).

3.2 JUC Spray Dressing reduces colonic bacterial biofilms

We performed quantitative analysis of SEM images using ImageJ to calculate the proportion of mucosal surface area covered by biofilm in each group, and compared groups using one–way ANOVA with *post hoc* testing (Figure 2B) with consistent magnification and random field selection. The JUC group exhibited a significantly lower biofilm coverage ratio than the DSS +PBS group.

Scanning electron microscopy (SEM) was employed to evaluate the effect of JUC Spray Dressing on intestinal bacterial biofilms. In the DSS+PBS group, SEM revealed biofilms in all 9/9 images. In contrast, biofilm coverage was markedly reduced in 8/9 images from the DSS+JUC group and in 6/9 images from the DSS+MTZ group. However, in the normal control group, the bacteria observed on the surface of the intestinal mucosa were found in planktonic form. As shown in Figure 2, biofilm was widely present in the colons of UC model mice and was covered with a thick matrix. In addition to bacteria of various morphologies, many water channels were observed in the biofilms. Unlike in UC model mice, most of the bacteria in the intestinal mucosa of mice in the normal control group were present in planktonic form and biofilm formation was rare. Treatment with MTZ or 5-ASA thinned the EPS matrix and

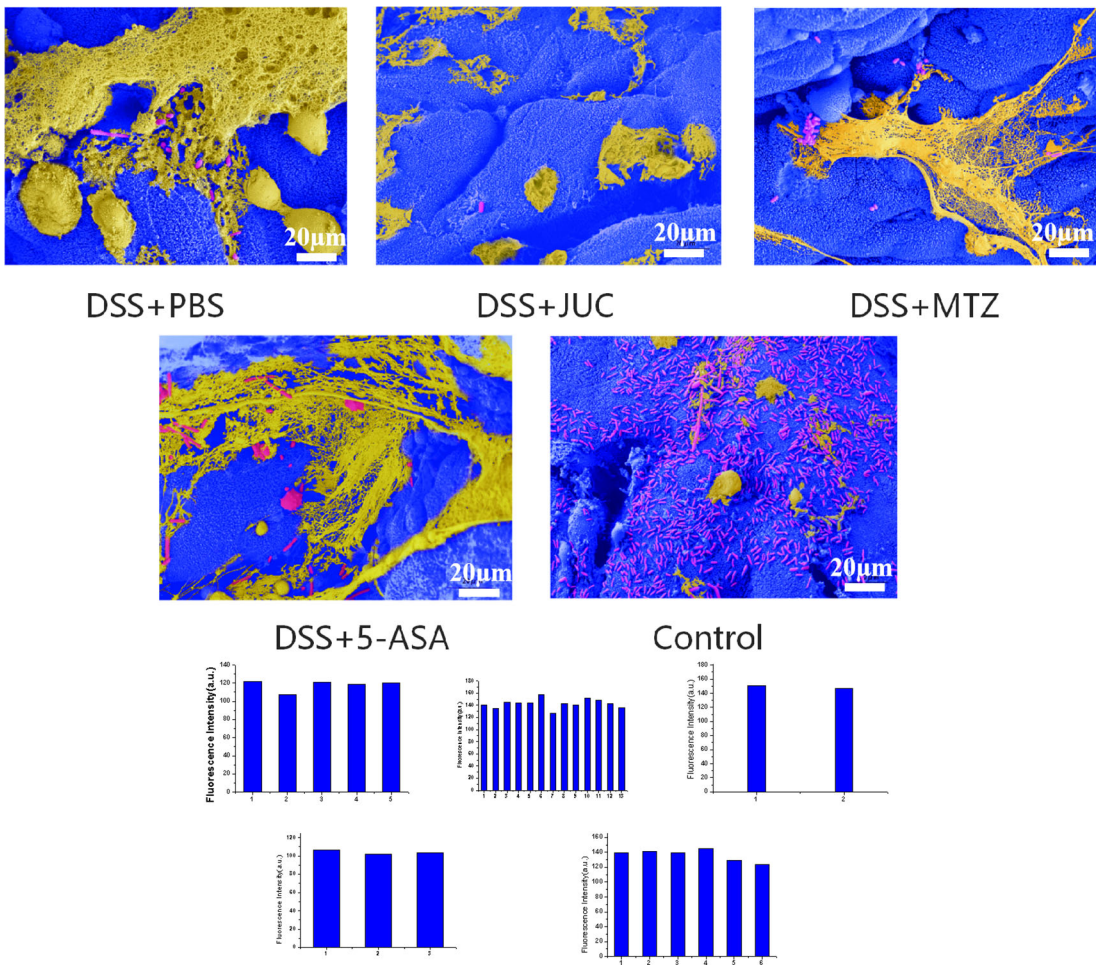

FIGURE 2
Bacterial biofilms on the intestinal mucosal surface, viewed by scanning electron microscopy(1000×). Quantification of biofilm coverage from SEM images. Biofilm-covered area was measured in ImageJ and expressed as the percentage of mucosal surface occupied by adherent biofilm. Bars show mean ± SD across animals; fields were randomly selected at the same magnification. One-way ANOVA with Tukey's *post hoc* test was used. Asterisks indicate significance vs DSS+PBS ($P<0.05$, *$P<0.01$, **$P<0.001$); brackets explicitly connect the compared groups.

the bacteria were exposed. Treatment with JUC Spray Dressing extensively reduced biofilm formation.

Quantitative SEM analysis (Figure 2B) demonstrated a significant reduction in biofilm-covered mucosal area in DSS +JUC versus DSS+PBS, consistent with visual thinning of extracellular polymeric substance (EPS) matrices and exposure of underlying bacteria. Biologically, decreased surface coverage by structured biofilms is expected to lessen epithelial PRR (e.g., TLR2/4) engagement and downstream NF-κB activation, aligning with the observed reductions in IL-6, TNF-α, and IL-1β and the improvements in tight-junction morphology and IF markers (MUC2, ZO-1, occludin).

3.3 JUC Spray Dressing decreases inflammatory cytokine production

Key pro-inflammatory cytokines associated with UC include IL-6, IL-1β, and TNF-α (21). ELISA was used to measure the level of inflammatory factors in serum and the immunohistochemistry results of end-colon tissue, as shown in Figure 3. Levels of IL-6, IL-1β, and TNF-α in the DSS+PBS group were significantly higher than those in the normal control group (P<0.0001). Following treatment with JUC Spray Dressing, MTZ, and 5-ASA enemas, IL-6 levels significantly decreased (P < 0.0001), along with reductions in TNF-α (P < 0.0001) and IL-1β (P < 0.001) levels. The differences among the three treatment groups were not statistically significant (P>0.05).

Quantitative IHC analysis in colon tissue showed trends consistent with serum ELISA, indicating concordant reductions in IL-6, IL-1β, and TNF-α across treatment groups.

3.4 JUC Spray Dressing improves intestinal barrier function

After DSS-induced UC, TEM revealed abnormal cell-to-cell connections, including the expansion of apical junction complexes and paracellular spaces. In the DSS+PBS group, the mucus layer was also damaged and thinned under the microscope, the apex was swollen and shedding, the arrangement was complex and sparse, and the organelles were swollen and necrotic. In contrast, the intestinal mucosal chorionic villi in the normal control group

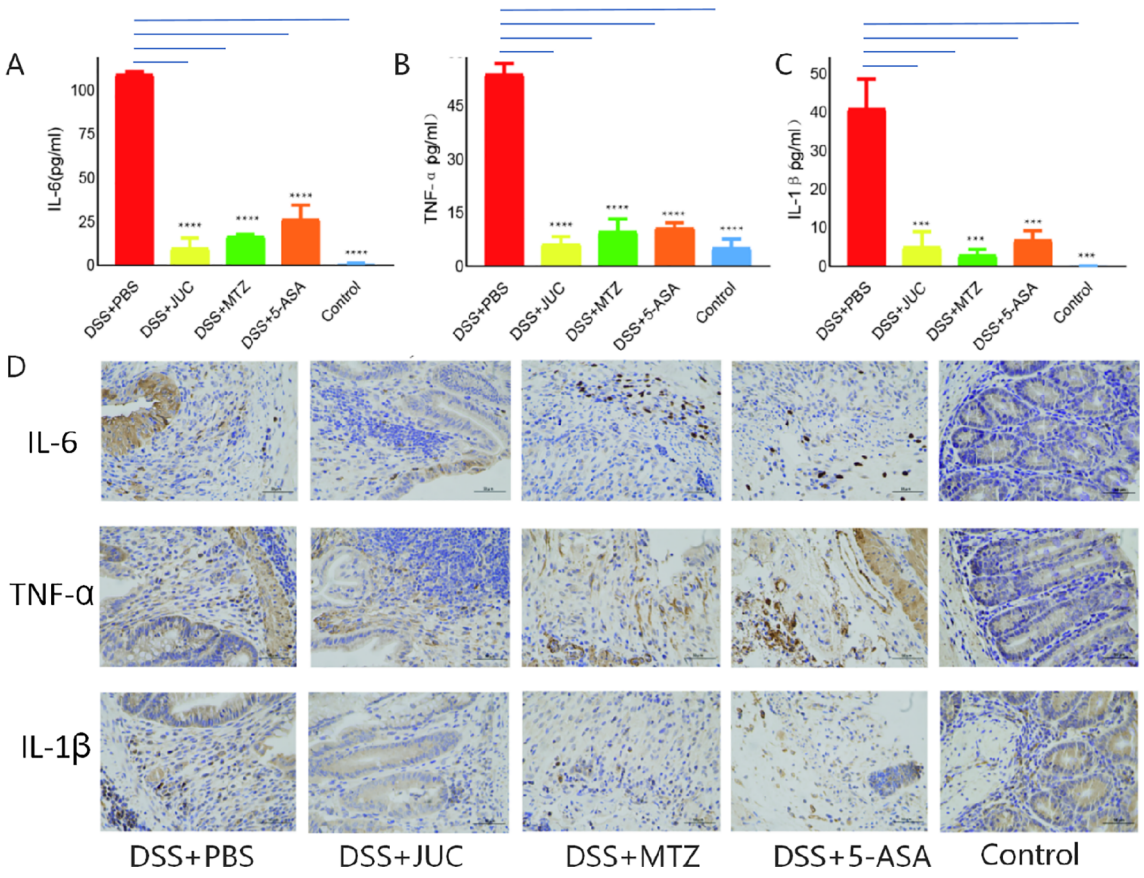

FIGURE 3
Effects of JUC Spray Dressing on the levels of inflammatory factors in peripheral blood. **(A)** Expression of IL-6 (N = 3). **(B)** Expression of TNF-α(N = 3) **(C)** Expression of IL-1β(N = 3),***P<0.001,****P<0.0001, compared to the DSS+PBS group. **(D)** Immunohistochemical analysis of inflammatory factors in the terminal colon(200×). Statistical analysis. Continuous multi-group comparisons of serum inflammatory cytokine levels (TNF-α, IL-6, IL-1β) were evaluated using Tukey's Honestly Significant Difference (HSD) test with multiple-comparison correction to assess pairwise differences among groups. A two-sided P < 0.05 was considered statistically significant.

were highly consistent and neatly arranged, the organelles were intact, and the cell connections were tight. Treatment with JUC, MTZ, and 5-ASA improved the abnormally tight cell junctions and cytoedema, and relieved barrier structural looseness caused by inflammation-induced TJ protein deletion (Figure 4A).

Mucin 2 (MUC2) is a high-molecular-weight glycoprotein secreted by epithelial cells, forming a protective mucus barrier in the intestine (8). After DSS-induced UC, the intestinal barrier of mice was damaged (Figure 4B) and the number of goblet cells was reduced (Figure 4C). TJs are an important part of the mucosal barrier, preventing harmful substances from leaking out of the intestinal lumen (22). The immunofluorescence analysis of MUC2 and TJ protein levels is shown in Figure 4D, the abundance of ZO-1 and occludin-positive cells was reduced in the DSS+PBS group compared to those in the normal control group, and the intestinal barrier function was impaired. The abundance of ZO-1- and occludin-positive cells was increased after JUC Spray Dressing, MTZ, and 5-ASA treatment, and the expression of MUC2 was increased in the JUC and 5-ASA groups, whereas MUC2 expression in the MTZ group was not significantly altered. Quantitative IF confirmed increased ZO−1 and occludin signals in all treatment groups versus DSS+PBS, with MUC2 increased in the JUC and 5 −ASA groups and not significantly changed in the MTZ group.

3.5 JUC Spray Dressing enhances intestinal microflora composition

We assessed α- and β-diversity by 16S rRNA sequencing of cecal contents. JUC increased α-diversity and shifted β-diversity relative to DSS+PBS, whereas phylum-level community composition did not change markedly (Figure 5), suggesting restoration of community evenness without wholesale restructuring. This pattern is compatible with selective biofilm disruption and reduced inflammatory drive rather than broad microbiota depletion. Because 16S profiling was performed on cecal contents rather than mucosa-associated communities, biofilm-resident taxa may be under-represented; future studies will sample mucosal layers (e.g., scrapings/biopsies) and apply FISH-based spatial analyses to capture biofilm-associated shifts more directly.

To assess the impact of JUC Spray Dressing on intestinal microbiota composition, 16S rRNA sequencing was conducted on mouse cecal contents, with six samples per group analyzed for operational taxonomic unit (OTU) distribution, as illustrated in the Venn diagram (Figure 5A). Overall, 926 OTUs were detected among the five groups, including 61, 130, 111, 93, and 227 OTUs in the DSS+PBS, DSS+JUC, DSS+MTZ, DSS + 5-ASA, and normal control groups, respectively.

Beta (β) diversity is mainly based on the OTU sequence similarity or community structure and is used to compare differences between populations. Intestinal flora diversity of mice was determined using principal coordinate analysis method and heat maps were constructed. Compared with the bacterial community of mice in the normal control group, the bacterial community of mice in the DSS+PBS group exhibited obvious isolation. The β diversity of the microbial community was increased to varying degrees after JUC Spray Dressing, MTZ, or 5-ASA treatment (Figure 5B). Alpha (α) diversity can be used to assess species richness and distribution. As shown in Figure 5C, the α-diversity correlation violin plot revealed the degree of sample dispersion within each group and the differences in α-diversity between treatment groups. α-Diversity was significantly lower in the DSS+PBS group than in the normal control group. However, α-diversity was significantly increased in the DSS+JUC and DSS +MTZ groups compared to the DSS+PBS group ($P < 0.05$). The α-diversity of the DSS + 5-ASA group did not differ significantly from that of the DSS+PBS group ($P>0.05$).

The histogram of the community structure (Figure 5D) demonstrated a decrease in bacterial diversity and an increase in the relative abundance of *Clostridium* spp. in the DSS+PBS group compared to those in the normal control group. The community structures did not differ significantly between the DSS+JUC and DSS+PBS groups.

At the phylum level, community composition did not differ significantly between the DSS+JUC and DSS+PBS groups, while α– and β–diversity indices increased after JUC treatment.

Heat maps at the genus level illustrated that probiotics species such as *Roseburia* and *Butyricimonas* were relatively more abundant in the normal control group than in the other groups. The relative abundance of probiotics species was reduced in the DSS+PBS group compared to that in the other groups, whereas the relative abundances of the gengra *Bacteroides and Dorea*, and anaerobic bacteria were higher. Additionally, the relative abundance of anaerobic bacteria was decreased after treatment with JUC Spray Dressing (Figure 5E).

Taken together, these data indicate that JUC exerts a selective, biofilm-targeted effect that reduces putatively harmful taxa (e.g., Bacteroides spp.) while maintaining overall community structure, a profile consistent with ecological stability rather than broad microbiota depletion.

4 Discussion

This study utilized a DSS-induced mouse model of UC to evaluate the therapeutic effects of JUC Spray Dressing (23). After administration of DSS for 7 days, mice in the DSS group exhibited a significant decrease in activity, weight loss, purulent diarrhea,and bloody stools. Elevated serum levels of inflammatory factors, structural disturbances of the colon glands, shedding and necrosis of the intestinal mucosa, extensive inflammatory cell infiltration, and typical crypt abscess formation demonstrated successful induction of enteritis in mice; thus, the mouse model effectively mimicked clinical UC (24).

Beyond global PRR–NF-κB attenuation, species-specific interactions and cellular targets (e.g., macrophage subsets, Th17 cells) warrant direct testing using gnotobiotic or defined-consortium models and epithelial/immune co-culture systems to delineate molecular mechanisms and specificity.

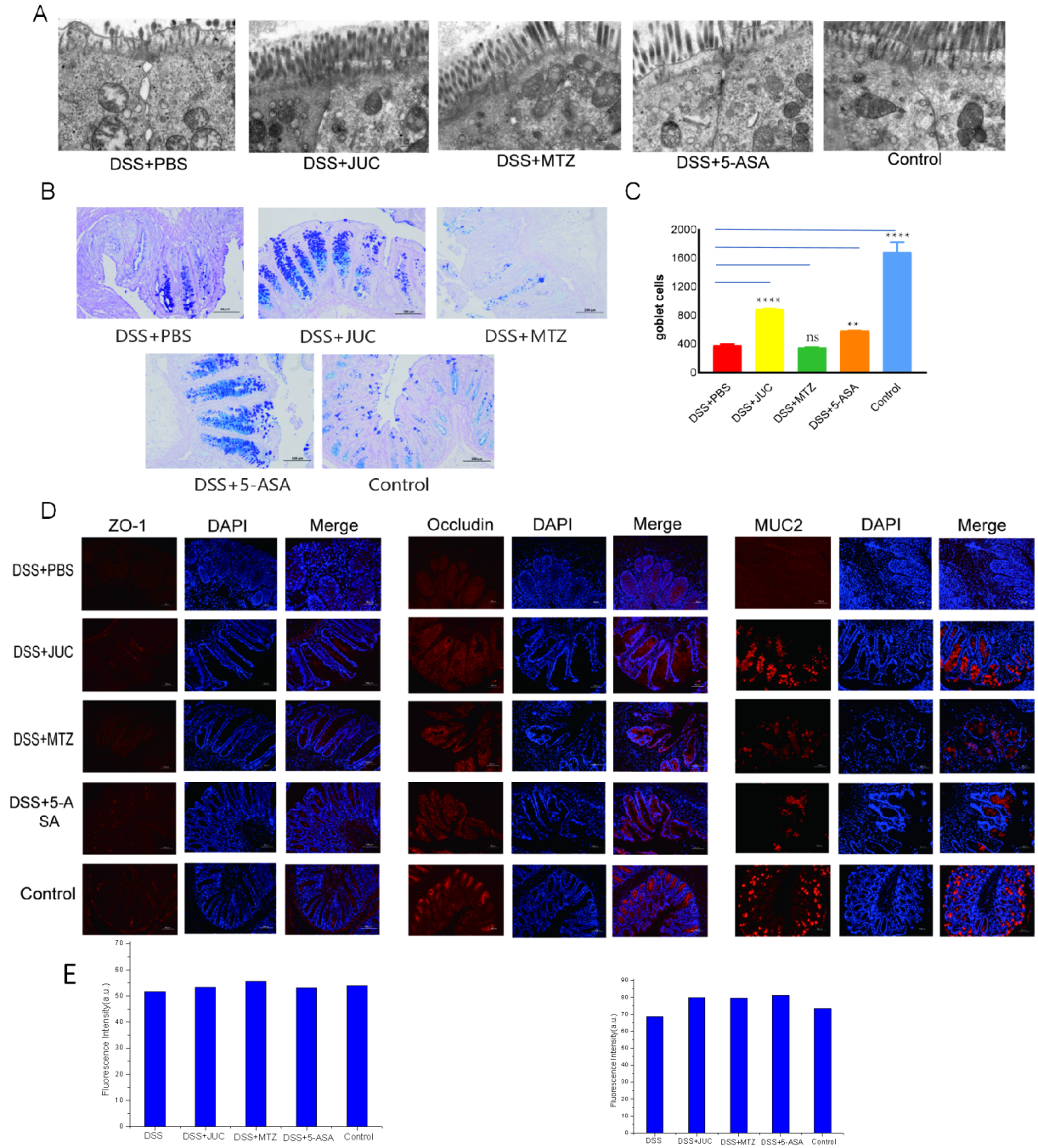

FIGURE 4
Effects of JUC Spray Dressing on the intestinal barrier function. **(A)** Intestinal mechanical barrier, viewed by transmission electron microscopy. **(B)** Periodic acid-Schiff (PAS)−Alcian blue (AB) stainingof the distal colon(200×). **(C)** Goblet cell count. **(D)** Immunofluorescence analysis of MUC2, ZO-1, occludin(200×). **(E)** Quantification of epithelial barrier markers by immunofluorescence (MUC2, ZO-1, and occludin). Signals were measured as mean fluorescence intensity in ImageJ. Bars show mean ± SD across animals; fields were randomly selected under identical imaging settings. One-way ANOVA with Tukey's *post hoc* test was used. Asterisks indicate significance vs DSS+PBS (P<0.05, *P<0.01, **P<0.001); brackets explicitly connect the compared groups. Statistical analysis and image quantification. Microscopy images were processed in ImageJ for automated cell counting; counts were based on immunofluorescence-positive cells defined by the specified markers. Continuous multi-group comparisons were evaluated using Tukey's Honestly Significant Difference (HSD) test with multiple-comparison correction to assess pairwise differences among groups. A two-sided P < 0.05 was considered statistically significant.

All three therapeutic agents tested in this study significantly reduced the expression of inflammatory cytokines in DSS-induced colitis, demonstrating their efficacy in mitigating experimental colitis. 5-ASA, which has similar molecular targets as non-steroidal anti-inflammatory drugs (NSAIDs), can inhibit intestinal inflammation and cell proliferation and apoptosis by inhibiting cyclooxygenase(COX) and prostaglandin(PGI). Thus, 5-ASA has been widely used to improve intestinal inflammation and prevent

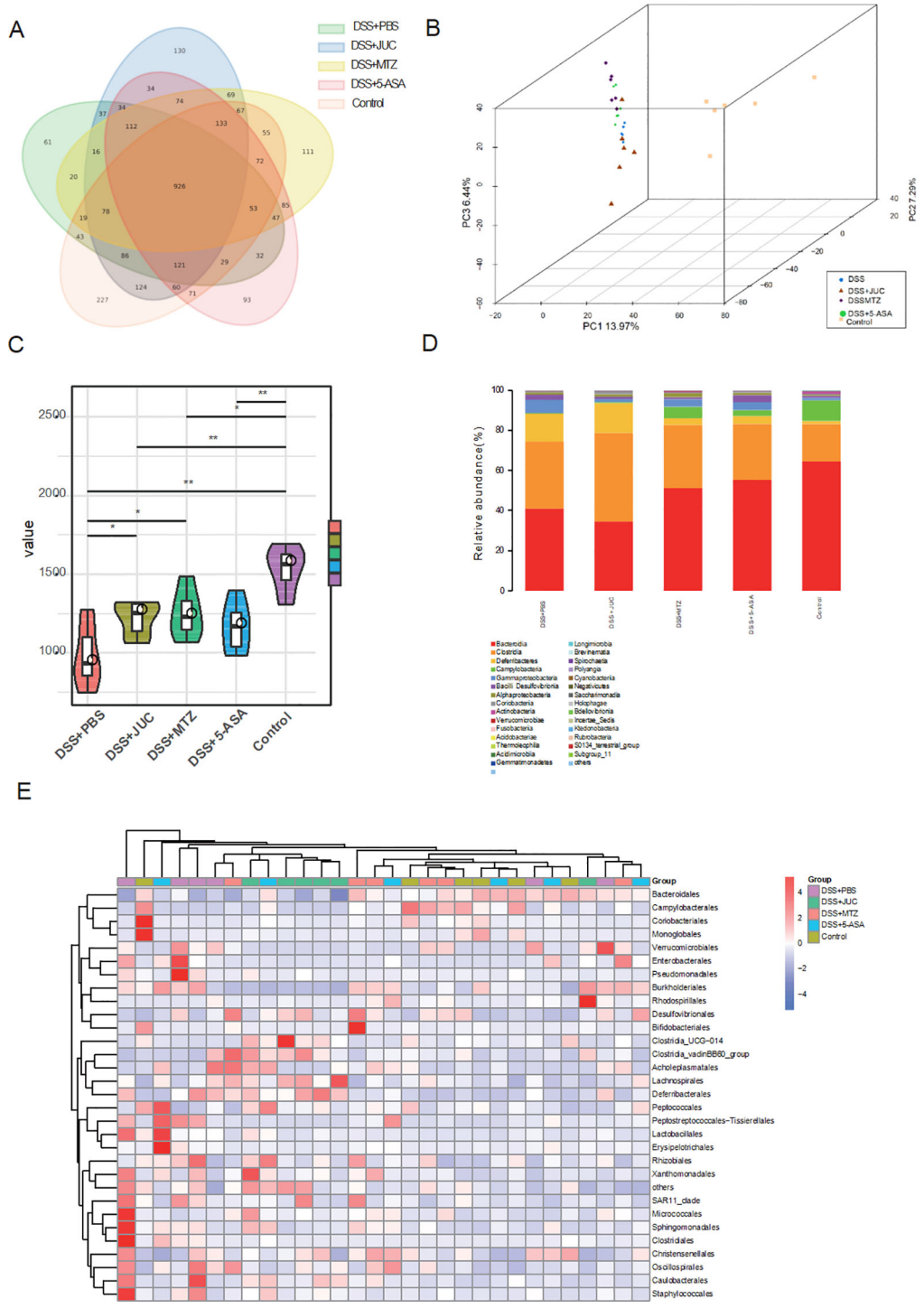

FIGURE 5
Changes in intestinal flora. **(A)** Venn diagram. **(B)** β diversity analysis. **(C)** α-diversity analysis. *P<0.05,**P<0.01, compared to the DSS+PBS group. **(D)** Histogram of the community structure. **(E)** Heat map.

tumorigenesis. Dahl et al. reported that 5-ASA can reduce intracellular polyphosphate levels in many bacteria, making bacteria sensitive to oxygenation stress and thereby reducing colonization and biofilm formation (25). The findings in the current study confirmed that 5-ASA has a certain clearance effect on colon biofilms while improving enteritis in mice. Currently, no studies have reported a direct relationship between QAS, COX, and PGI. Therefore, the exact mechanism by which QAS improves inflammation warrants further investigation. It has been suggested that narrow-spectrum antibiotics in patients with IBD do not achieve the same effect as broad-spectrum antibiotics, suggesting that reducing the colonic bacterial load in patients with IBD may

control disease activity (26, 27). According to the results of the current study, both broad-spectrum antimicrobials and physical sterilization with JUC Spray Dressing effectively alleviated experimental colitis in mice by reducing the bacterial load of the colon.

Mechanistically, clearance of biofilms is expected to reduce engagement of epithelial and immune pattern-recognition receptors (PRRs), particularly TLR2/TLR4, thereby dampening NF-κB activation and downstream production of IL-6, TNF-α, and IL-1β. In addition, attenuated TLR/NF-κB signaling may shift mucosal immune balance by limiting pro-inflammatory macrophage activation and constraining Th17 responses; these hypotheses merit direct testing in future work. It also remains unclear whether biofilm formation in UC is a cause or a consequence of mucosal inflammation. These processes may be bidirectionally causal, forming a positive feedback loop in which inflammation facilitates biofilm formation while biofilms further amplify inflammatory signaling; establishing directionality will require longitudinal and interventional studies.

JUC Spray Dressing kills bacteria via electrostatic interactions, thereby minimizing the risk of inducing antimicrobial resistance. A previous study reported that JUC Spray Dressing was effective against a wide variety of microorganisms (17). Acute oral tests in mice showed that JUC Spray Dressing is safe and non-toxic, and JUC Spray Dressing has been widely adopted for skin and wound detoxification and indwelling catheter care (16). These results suggested that JUC Spray Dressing could improve experimental colitis in mice by reducing colonic biofilm formation.

Patients with IBD exhibit increased intestinal permeability, facilitating bacterial translocation and microbial dysbiosis (28). Although it is generally believed that the intestinal flora is involved in the pathogenesis of IBD, most studies have focused on changes in microflora abundance while ignoring the spatial structure of the biofilm (29, 30). Intestinal mucosal biofilms are significantly more abundant in patients with IBD than in healthy subjects, and gut bacteria are more likely to colonize and form biofilms in these patients, leading to inflammation (31, 32). High concentrations of bacteria, similar to those found in biofilms, can lead to high levels of local bacterial antigens, toxins, or other harmful substances (33). Therefore, treatments that target biofilms can improve intestinal inflammation. Meanwhile, intestinal barrier dysfunction is one of the main pathological features of UC (34). Intestinal epithelial cells are covered with mucus secreted by goblet cells, which prevents bacterial invasion (35, 36). TJs between intestinal epithelial cells provide a barrier to the free diffusion of substances and prevent the transposition of intestinal pro-inflammatory substances into the bloodstream (37). The current study findings demonstrated that JUC Spray Dressing can enhance intestinal barrier function, which may be related to its ability to effectively reduce the bacterial load of the colon and promote ulcer healing.

A previous study hypothesized that UC is a disease associated with microbial infections (38). Biofilms formed by large bacterial communities can enhance the penetration of bacteria, destroying the barrier function of the mucus layer. Bacteria come into direct contact with epithelial cells through the sterile mucus layer, causing an abnormal immune response that leads to the development and progression of various diseases (39). A previous study demonstrated that biofilms were found more often in intestinal mucosal biopsy specimens in patients with IBD than healthy individuals (31). In the current study, SEM revealed a larger, richer, and thicker intestinal biofilm in the DSS+PBS group and a variety of channels in the internal structure of the biofilm. Various forms of bacteria can exchange information and nutrients within the biofilm, and a small number of symbiotic bacteria can also form biofilms to enhance interactions with the host (6). Indeed, most of the gut bacteria in the normal control group were present in plank tonic form. However, MTZ or 5-ASA thinned the matrix to varying degrees, exposing the bacteria within the biofilm. Meanwhile, JUC reduced biofilm formation and bacterial abundance over a large area and significantly thinned the matrix, indicating that JUC Spray Dressing can effectively target colonic bacterial biofilms.

Considering the non-specificity of physical sterilization by JUC, 16S rDNA sequencing analysis of mouse ileocecal contents was further performed to explore the effect on intestinal flora composition. The intestinal flora of mice in the DSS+PBS group was dysregulated with low intestinal flora diversity. Meanwhile, the intestinal flora of the DSS+JUC group presented greater α and β diversity than that of the DSS+PBS group, as did that of the DSS +MTZ and DSS + 5-ASA groups. However, the community structure of the intestinal flora was not significantly altered, indicating that JUC Spray Dressing did not significantly affect the composition of the intestinal microbiota. Nevertheless, the content of the cecum,which was not affected by the enema operation, was employed in the current study to analyze the microflora of the mice. Therefore, changes in the mucosal flora should be clarified in future experiments. Overall, compared to MTZ and 5-ASA therapy, which can lead to increased drug resistance, opportunistic infections, and liver and kidney function impairment, JUC Spray Dressing may provide a safe treatment option for UC.

At present, the principles of biofilm intervention mainly include inhibiting adhesion, interfering with the group sensing system among bacteria, promoting biofilm separation (returning bacteria to a planktonic state), destroying the protective screen barrier through mechanical and physical means, and promoting the colonization of probiotics to achieve competitive inhibition (40, 41). As EPS is a protective barrier to biofilm formation, new therapeutic strategies can also inhibit biofilm growth by targeting the destruction of EPS. Surfactants with an electrically charged surface, such as citric acid amphoteric surfactants, can chelate the calcium ion bridge in EPS, making it less stable and easier to destroy (42). In addition, enzymatic digestion by proteases can disrupt biofilms. Patients with IBD have larger mucosal bacteria biofilms and higher iron concentrations within cells than healthy individuals; however, hydrogen sulfide derivatives can remove iron. Motta et al. reported that directly reducing the intake of microbial binders can reduce the ability of IBD-associated mucosal bacteria to form biofilms, without affecting the composition of the bacterial community, thereby improving dinitrobenzene sulfonic acid-induced enteritis in mice (13). The results of the current study

also indicated that JUC Spray Dressing reduced biofilm formation without affecting the composition of the bacterial community. However, unlike in previous studies where metal chelating agents destroyed the stability of EPS by directly chelating metal ions, JUC Spray Dressing directly killed bacteria via electrostatic action to destroy the biological membrane. Whether combined use with JUC Spray Dressing can significantly enhance the effects of antibiotic treatment by destroying the protective barrier provided by the biofilm needs to be verified in the future. At the time of writing, obvious drug toxicity has not been reported for JUC Spray Dressing; therefore, further pharmacokinetic experiments are required to determine any potential toxic side effects. Further, whether JUC Spray Dressing is capable of preventing the occurrence of IBD in healthy individuals also warrants further study.

Previous research has linked biofilm formation to the pathogenesis of various diseases, including Barrett's esophagus, familial adenomatous polyposis, and colorectal cancer (43, 44). Whether targeting biofilms can improve or intervene in the progression of these diseases requires further study. In addition, the anatomy of the mouse intestine differs from that of humans—mice do not have an appendix and the cecum is enlarged—and some studies have proposed that the human appendix plays an important role in the reconstruction of the gut flora after antibiotic use. Thus, while mouse models are extensively utilized in gut microbiome research, replicating the complexity of the human intestinal microbiota remains challenging (45, 46). Finally, while SEM was utilized to visualize mucosal biofilms in this study, future research should incorporate advanced techniques such as three-dimensional (3D) imaging for quantifying biofilm thickness and density, as well as fluorescence *in situ* hybridization (FISH) probes for precise microbial identification.

Long-term implications: although JUC is bactericidal and not intended to increase probiotic taxa (e.g., Roseburia, Butyricimonas), the JUC group exhibited higher α- and β-diversity indices relative to DSS+PBS with only modest phylum-level shifts, consistent with restoration of community evenness rather than wholesale taxonomic restructuring. By selectively disrupting biofilms and reducing inflammatory drive while preserving overall community structure, JUC may lower the inflammatory set-point and strengthen epithelial barrier resilience. In contrast, MTZ can induce broader compositional perturbations and 5-ASA, while anti-inflammatory, does not directly target biofilms. Thus, potential long-term benefit may derive from reduced harmful stimuli and maintained stability rather than direct enrichment of specific probiotic taxa; validation in chronic/relapsing models and functional readouts (e.g., short-chain fatty acid profiling) is warranted. This pattern suggests functional selectivity—targeting biofilm-associated states and inflammatory drive—rather than taxonomic over-pruning. In contrast to MTZ, which often induces broader compositional shifts, JUC's preservation of overall structure with increased diversity may lower the inflammatory set-point with less risk of dysbiosis over time. Nonetheless, long-term ecological consequences require longitudinal sampling and functional readouts (e.g., short-chain fatty acids, mucus barrier function), ideally including mucosa-associated 16S/shotgun profiling to resolve biofilm-resident species-level selectivity.

Safety and pharmacokinetics: this exploratory study did not include mucosal toxicology, pharmacokinetic, or intraluminal retention analyses for JUC after colonic application. Accordingly, statements regarding safety and local exposure are presented as hypotheses; future work will quantify luminal and tissue concentrations, residence time, and mucosal penetration, alongside formal toxicology.

Limitations: first, the sample size was limited and the study may have been underpowered to detect subtle inter-treatment differences; we therefore used cautious language when comparing JUC with MTZ and 5-ASA. The study was conducted once with n=10 per group, which limits statistical power and external validity; the findings should be viewed as preliminary. Replication in independent cohorts and prespecified power calculations will be incorporated in follow-up studies. Second, we did not perform direct barrier-function assays (e.g., FITC-dextran permeability); our barrier conclusions are based on structural and protein-level readouts and should be validated by functional testing. Third, although we quantified biofilm coverage by image analysis (Figure 2B), standardized multicenter pipelines for biofilm metrics would strengthen generalizability.

Outlook: because DSS primarily models acute colitis, future work will evaluate JUC Spray Dressing in chronic and relapsing models to better approximate long–term disease dynamics and therapeutic responses.

5 Conclusions

This study evaluated the therapeutic effects of an Organosilicone Double-Long-Chain Diquaternary Ammonium Salt formulation, represented by JUC Spray Dressing, in a DSS-induced mouse model of colitis, comparing its efficacy with conventional treatments such as MTZ and 5-ASA. The results suggest that JUC efficacy is comparable to conventional treatments, suggesting its potential as an alternative therapeutic option for UC, and larger studies are required to validate this comparability. The findings of this study further support the hypothesis that microbial infections contribute to the pathogenesis of UC and that controlling bacterial biofilm formation may alleviate intestinal inflammation. These findings provide valuable insights into the potential clinical applications of Organosilicone Double-Long-Chain Diquaternary Ammonium Salts in UC management.

Data availability statement

The original contributions presented in the study are included in the article/supplementary material. Further inquiries can be directed to the corresponding author.

Ethics statement

The animal study was approved by Animal Ethics Committee of the General Hospital of Eastern Theater Command. The study was conducted in accordance with the local legislation and institutional requirements.

Author contributions

SPS: Writing – original draft. GT: Writing – original draft. JW: Writing – review & editing. SS: Writing – review & editing. ZD: Writing – review & editing. QA: Writing – review & editing. HT: Writing – review & editing. FW: Writing – review & editing.

Funding

The author(s) declare that financial support was received for the research and/or publication of this article. This study was supported by the National Science Foundation of China (No. 81873559; No. 82170574).

Acknowledgments

We thank Professor Fangyu Wang for his careful guidance and help. Thanks to NMS Technologies Co., Ltd. for the technical guidance.

Conflict of interest

The authors declare that the research was conducted in the absence of any commercial or financial relationships that could be construed as a potential conflict of interest.

Generative AI statement

The author(s) declare that no Generative AI was used in the creation of this manuscript.

Any alternative text (alt text) provided alongside figures in this article has been generated by Frontiers with the support of artificial intelligence and reasonable efforts have been made to ensure accuracy, including review by the authors wherever possible. If you identify any issues, please contact us.

Publisher's note

References

1. Fodil N, Moradin N, Leung V, Olivier JF, Radovanovic I, Jeyakumar T, et al. CCDC88Bis required for pathogenesis of inflammatory bowel disease. *Nat Commun*. (2017) 8:932. doi: 10.1038/s41467-017-01381-y

2. Rubin SJS, Bai L, Haileselassie Y, Garay G, Yun C, Becker L, et al. Mass cytometry reveals systemic and local immune signatures that distinguish inflammatory bowel diseases. *Nat Commun*. (2019) 10:2686. doi: 10.1038/s41467-019-10387-7

3. Mcgovern DP, Kugathasan S, Cho JH. Genetics of inflammatory boweldiseases. *Gastroenterology*. (2015) 149:1163–76.e2. doi: 10.1053/j.gastro.2015.08.001

4. Wlodarska M, Kostic AD, Xavier RJ. An integrative view of microbiome-host interactions in inflammatory bowel diseases. *Cell Host Microbe*. (2015) 17:577–91. doi: 10.1016/j.chom.2015.04.008

5. Schwerd T, Bryant RV, Pandey S, Capitani M, Meran L, Cazier JB, et al. NOX1 loss-of-function genetic variants in patients with inflammatory bowel disease. *Mucosal Immunol*. (2018) 11:562–74. doi: 10.1038/mi.2017.74

6. Motta JP, Wallace JL, Buret AG, Deraison C, Vergnolle N. Gastrointestinal biofilms in health and disease. *Nat Rev Gastroenterol Hepatol*. (2021) 18:314–34. doi: 10.1038/s41575-020-00397-y

7. Parsek MR, Fuqua C. Biofilms2003: emerging themes and challenges in studies of surface-associated microbial life. *J Bacteriol*. (2004) 186:4427–40. doi: 10.1128/JB.186.14.4427-4440.2004

8. Breugelmans T, Van Spaendonk H, De Man JG, De Schepper HU, Jauregui-Amezaga A, Macken E, et al. In-Depth Study of transmembrane mucins in association with intestinal barrier dysfunction during the course of T cell transfer and DSS-induced colitis. *J Crohns Colitis*. (2020) 14:974–94. doi: 10.1093/ecco-jcc/jjaa015

9. Bantel H, Berg C, Vieth M, Stolte M, Kruis W, Schulze-Osthoff K. Mesalazine inhibits activation of transcription factor NF-kappaB in inflamed mucosa of patients with ulcerative colitis. *Am J Gastroenterol*. (2000) 95:3452–7. doi: 10.1111/j.1572-0241.2000.03360.x

10. Ohkusa T, Kato K, Terao S, Chiba T, Mabe K, Murakami K, et al. Newly developed antibiotic combination therapy for ulcerative colitis: a double-blind placebo-controlled multicenter trial. *Am J Gastroenterol*. (2010) 105:1820–9. doi: 10.1038/ajg.2010.84

11. Panpetch W, Hiengrach P, Nilgate S, Tumwasorn S, Somboonna N, Wilantho A, et al. Additional Candida albicans administration enhances the severity of dextran sulfate solution induced colitis mouse model through leaky gut-enhanced systemic inflammation and gut-dysbiosis but attenuated by Lactobacillus rhamnosusL34. *Gut Microbes*. (2020) 11:465–80. doi: 10.1080/19490976.2019.1662712

12. Rao K, Higgins PD. Epidemiology, diagnosis, and management of Clostridium difficile infection in patients with inflammatory boweldisease. *Inflammation Bowel Dis*. (2016) 22:1744–54. doi: 10.1097/MIB.0000000000000793

13. Motta JP, Allain T, Green-Harrison LE, Groves RA, Feener T, Ramay H, et al. Iron sequestration in microbiota biofilms as a novel strategy for treating inflammatory bowel disease. *Inflammation Bowel Dis*. (2018) 24:1493–502. doi: 10.1093/ibd/izy116

14. Motta JP, Flannigan KL, Agbor TA, Beatty JK, Blackler RW, Workentine ML, et al. Hydrogen sulfide protects from colitis and restores intestinal microbiota biofilm and mucus production. *Inflammation Bowel Dis*. (2015) 21:1006–17. doi: 10.1097/MIB.0000000000000345

15. Zhou H, Weir MD, Antonucci JM, Schumacher GE, Zhou XD, Xu HH. Evaluation of three-dimensional biofilms on antibacterial bonding agents containing novel quaternary ammonium methacrylates. *Int J Oral Sci*. (2014) 6:77–86. doi: 10.1038/ijos.2014.18

16. Cheng L, Weir MD, Zhang K, Xu SM, Chen Q, Zhou X, et al. Antibacterial nanocomposite with calcium phosphate and quaternary ammonium. *J Dent Res*. (2012) 91:460–6. doi: 10.1177/0022034512440579

17. Wu J, Zhou H, Weir MD, Melo MA, Levine ED, Xu HH. Effect of dimethylaminohexadecyl methacrylate mass fraction on fracture toughness and antibacterial properties of CaP nanocomposite. *J Dent*. (2015) 43:1539–46. doi: 10.1016/j.jdent.2015.09.004

18. Wirtz S, Popp V, Kindermann M, Gerlach K, Weigmann B, Fichtner-Feigl S, et al. Chemically induced mouse models of acute and chronic intestinal inflammation. *Nat Protoc*. (2017) 12:1295–309. doi: 10.1038/nprot.2017.044

19. Lee JG, Lee YR, Lee AR, Park CH, Han DS, Eun CS. Role of the global gut microbial community in the development of colitis-associated cancer in a murine model. *BioMed Pharmacother*. (2021) 135:111206. doi: 10.1016/j.biopha.2020.111206

20. Lin JC, Wu JQ, Wang F, Tang FY, Sun J, Xu B, et al. QingBai decoction regulates intestinal permeability of dextran sulphate sodium-induced colitis through the modulation of notch and NF-κB signalling. *Cell Prolif*. (2019) 52:e12547. doi: 10.1111/cpr.12547

21. Perey AC, Weishaar IM, Mcgee DW. The effect of ROCK on TNF-α-induced CXCL8 secretion by intestinal epithelial cell lines is mediated through MKK4 and JNK signaling. *CellImmunol*. (2015) 293:80–6. doi: 10.1016/j.cellimm.2014.12.011

22. Zuo L, Kuo WT, Turner JR. Tight junctions as targets and effectors of mucosalimmunehomeostasis. *Cell Mol Gastroenterol Hepatol*. (2020) 10:327–40. doi: 10.1016/j.jcmgh.2020.04.001

23. Nakakura S, Matsui M, Sato A, Ishii M, Endo K, Muragishi S, et al. Pathophysiological significance of the two-pore domain K(+) channel K2P5.1 in splenic CD4(+)CD25(-) T cell subset from a chemically-induced murine inflammatory bowel disease model. *Front Physiol*. (2015) 6:299. doi: 10.3389/fphys.2015.00299

24. Chassaing B, Aitken JD, Malleshappa M, Vijay-Kumar M. Dextran sulfate sodium (DSS)-induced colitis in mice. *CurrProtocImmunol*. (2014) 104:15–25. doi: 10.1002/0471142735.im1525s104

25. Dahl JU, Gray MJ, Bazopoulou D, Beaufay F, Lempart J, Koenigsknecht MJ, et al. The anti-inflammatory drug mesalamine targets bacterial polyphosphate accumulation. *Nat Microbiol*. (2017) 2:16267. doi: 10.1038/nmicrobiol.2016.267

26. Ohkusa T, Nomura T, Terai T, Miwa H, Kobayashi O, Hojo M, et al. Effectiveness of antibiotic combination therapy in patients with active ulcerative colitis: a randomized, controlled pilot trial with long-term follow-up. *Scand J Gastroenterol*. (2005) 40:1334–42. doi: 10.1080/00365520510023648

27. Wang SL, Wang ZR, Yang CQ. Meta-analysis of broad-spectrum antibiotic therapy in patients with active inflammatory bowel disease. *ExpTherMed*. (2012) 4:1051–6. doi: 10.3892/etm.2012.718

28. Bussières-Marmen S, Vinette V, Gungabeesoon J, Aubry I, Pérez-Quintero LA, Tremblay ML. Loss of T-cell protein tyrosine phosphatase in the intestinal epithelium promotes local inflammation by increasing colonic stem cell proliferation. *CellMolImmunol*. (2018) 15:367–76. doi: 10.1038/cmi.2016.72

29. Bottery MJ, Passaris I, Dytham C, Wood AJ, van der Woude MW. Spatial organization of expanding bacterial colonies is affected by contact-dependent growth inhibition. *Curr Biol*. (2019) 29:3622–3634.e5. doi: 10.1016/j.cub.2019.08.074

30. Qiu X, Zhao X, Cui X, Mao X, Tang N, Jiao C, et al. Characterization of fungal and bacterial dysbiosis in young adult Chinese patients with Crohn's disease. *Therap Adv Gastroenterol*. (2020) 13:1756284820971202. doi: 10.1177/1756284820971202

31. Swidsinski A, Weber J, Loening-Baucke V, Hale LP, Lochs H. Spatial organization and composition of the mucosal flora in patients with inflammatory bowel disease. *J Clin Microbiol*. (2005) 43:3380–9. doi: 10.1128/JCM.43.7.3380-3389.2005

32. Ellermann M, Sartor RB. Intestinal bacterial biofilms modulate mucosal immune responses. *J Immunol Sci*. (2018) 2:13–8. doi: 10.29245/2578-3009/2018/2.1122

33. Antón M, Rodríguez-González A, Ballesta A, González N, Del Pozo A, de Fonseca FR, et al. Alcohol binge disrupts the rat intestinal barrier: the partial protective role of oleoylethanolamide. *Br J Pharmacol*. (2018) 175:4464–79. doi: 10.1111/bph.14501

34. Sun X, Yang Q, Rogers CJ, Du M, Zhu MJ. AMPK improves gut epithelial differentiation and barrier function via regulating Cdx2 expression. *Cell Death Differ*. (2017) 24:819–31. doi: 10.1038/cdd.2017.14

35. Bergström JH, Birchenough GM, Katona G, Schroeder BO, Schütte A, Ermund A, et al. Gram-positive bacteria are held at a distance in the colon mucus by the lectin-like protein ZG16. *Proc Natl Acad Sci USA*. (2016) 113:13833–8. doi: 10.1073/pnas.1611400113

36. Donaldson GP, Lee SM, Mazmanian SK. Gut biogeography of the bacterial microbiota. *Nat Rev Microbiol*. (2016) 14:20–32. doi: 10.1038/nrmicro3552

37. Ma Y, Yue J, Zhang Y, Shi C, Odenwald M, Liang WG, et al. ACF7 regulates inflammatory colitis and intestinal wound response by orchestrating tight junction dynamics. *Nat Commun*. (2017) 8:15375. doi: 10.1038/ncomms15375

38. Ohkusa T, Koido S. Intestinal microbiota and ulcerative colitis. *J Infect Chemother*. (2015) 21:761–8. doi: 10.1016/j.jiac.2015.07.010

39. Bell A, Brunt J, Crost E, Vaux L, Nepravishta R, Owen CD, et al. Elucidation of a sialic acid metabolism pathway in mucus-foraging Ruminococcusgnavus unravels mechanisms of bacterial adaptation to the gut. *NatMicrobiol*. (2019) 4:2393–404. doi: 10.1038/s41564-019-0590-7

40. Kimyon Ö, Das T, Ibugo AI, Kutty SK, Ho KK, Tebben J, et al. Serratia secondary metabolite prodigiosin inhibits pseudomonas aeruginosa biofilm development by producing reactive oxygen species that damage biological molecules. *Front Microbiol*. (2016) 7:972. doi: 10.3389/fmicb.2016.00972

41. Hughes G, Webber MA. Novel approaches to the treatment of bacterial biofilm infections. *Br J Pharmacol*. (2017) 174:2237–46. doi: 10.1111/bph.13706

42. Motta JP, Denadai-Souza A, Sagnat D, Guiraud L, Edir A, Bonnart C, et al. Active thrombin produced by the intestinal epithelium controls mucosal biofilms. *Nat Commun*. (2019) 10:3224. doi: 10.1038/s41467-019-11140-w

43. Chew SS, Tan LT, Law JW, Pusparajah P, Goh BH, Ab Mutalib NS, et al. Targeting gut microbial biofilms-a key to hinder colon carcinogenesis? *Cancers*. (2020) 12:2272. doi: 10.3390/cancers12082272

44. Dejea CM, Fathi P, Craig JM, Boleij A, Taddese R, Geis AL, et al. Patients with familial adenomatous polyposis harbor colonic biofilms containing tumorigenic bacteria. *Science*. (2018) 359:592–7. doi: 10.1126/science.aah3648

45. Fessler J, Matson V, Gajewski TF. Exploring the emerging role of the microbiome in cancer immunotherapy. *JImmunotherCancer*. (2019) 7:108. doi: 10.1186/s40425-019-0574-4

46. Parian A, Limketkai B, Koh J, Brant SR, Bitton A, Cho JH, et al. Appendectomy does not decrease the risk of future colectomy in UC: results from a large cohort and meta-analysis. *Gut*. (2017) 66:1390–7. doi: 10.1136/gutjnl-2016-311550

《免疫学前沿》

类型 原创研究
发表 2025 年 12 月 12 日
DOI 10.3389/fimmu.2025.1644433

有机硅双长链双季铵盐作为生物膜清除剂改善葡聚糖硫酸钠诱导的结肠炎

史少培[1] ，唐国兴[2]，魏娟[2]，沈思[2]，丁志豪[2]，安琴[2]，陶辉[2]，汪芳裕[2]*

[1] 南京医科大学江宁医院肾内科
[2] 南京医科大学附属金陵医院/东部战区总医院消化科，南京，江苏，中国
通讯作者：汪芳裕
南京医科大学附属金陵医院/东部战区总医院消化科，中国江苏南京，邮编 210002

目的：溃疡性结肠炎（UC）因治疗效果有限且副作用显著，仍是临床难题。有机硅双长链二季铵盐（JUC 喷雾敷料）具有抗菌、抗炎及促进创面愈合的特性。本研究旨在评估 JUC 喷雾敷料在葡聚糖硫酸钠（DSS）诱导的 UC 小鼠模型中的治疗效果，并探讨其潜在作用机制。
方法：采用 3% DSS 建立小鼠 UC 模型，随后给予 JUC 喷雾敷料灌肠治疗。评估疾病活动指数（DAI）、组织学评分、肠黏膜细菌生物膜及紧密连接完整性。检测外周血炎性细胞因子水平，并进行 16S rDNA 扩增测序以分析盲肠微生物群组成。
结果：JUC 喷雾敷料可显著缓解 UC 症状，降低结肠充血程度，与其他治疗组相比差异无统计学意义（$P > 0.05$）。所有治疗均显著降低外周血炎性细胞因子的表达（$P < 0.0001$），组间差异无统计学意义。此外，各治疗组均有效减少生物膜厚度和细菌丰度，并改善肠屏障完整性。JUC 喷雾敷料能够抑制如拟杆菌属（Bacteroides spp.）等有害菌，但对整体微生物组成无显著影响。
结论：JUC 喷雾敷料可有效清除肠道细菌生物膜、降低炎症并增强屏障功能，从而改善 UC 症状。其疗效与常规治疗相当，具有作为替代治疗方案的潜力；但本研究未评估黏膜安全性，仍需专门的毒理学研究以确认其腔内使用的安全性。

关键词： 溃疡性结肠炎；细菌生物膜；有机硅双长链双季铵盐；治疗；结肠炎

1 引言

炎症性肠病（IBD）是一类胃肠道的慢性炎症性疾病，包括克罗恩病（CD）和溃疡性结肠炎（UC）(1)。随着中国快速工业化以及饮食模式的西方化，IBD 的发病率逐年上升，已成为常见的消化系统疾病之一 (2)。尽管 IBD 的确切发病机制尚未明确，但普遍认为与多种因素有关，包括遗传易感性、肠道屏障功能障碍以及肠道微生物群失衡等 (3–5)。大多数 IBD 患者存在复发—缓解交替的病程，且往往难以完全缓解。细菌生物膜被认为在 IBD 的发病中发挥关键作用 (6)。当细菌黏附于生物或非生物表面后，会分泌蛋白质和黏多糖，促进生物膜的形成，从而建立结构化的微生物群落。一旦生物膜成熟，其中的细菌能够脱落并扩散至新的部位，形成更多生物膜并持续造成慢性感染。生物膜内的细菌被包埋于胞外聚合物（EPS）基质

中，可形成保护屏障，提高其对外界压力的抵抗能力 (7)。在 IBD 患者中，肠道屏障受损，使细菌得以穿透黏液层并直接与肠上皮接触，从而促进生物膜形成并加重炎症。因此，在 IBD 患者肠黏膜中更易检测到生物膜的存在。

目前 IBD 的治疗手段包括 5-氨基水杨酸（5-ASA）、糖皮质激素、免疫抑制剂及生物制剂等，但其应用常受严重不良反应及高费用限制，亟需开发新的治疗策略 (8)。5-ASA 是一种结构类似乙酰水杨酸的抗炎药，其对 UC 的确切作用机制尚不明确，但研究认为其可抑制前列腺素和白三烯的生成，发挥抗炎作用。除此之外，5-ASA 还可抑制核因子 NF-κB，调节 PPAR-γ 受体，并抑制活性氧介导的肠黏膜 DNA 损伤 (9)。口服抗生素也可改善难治性 UC 的病程。阿莫西林、甲硝唑（MTZ）及环丙沙星等抗生素常被作为 IBD 的辅助治疗方案。在日本一项多中心随机试验中，接受联合抗生素治疗的 UC 患者获得了更有效的临床缓解和内镜愈合 (10)。然而，抗生素的使用会扰乱肠道细菌与真菌之间的平衡。尤其是白色念珠菌（Candida albicans），在肠道菌群紊乱后具有潜在致病作用，是 IBD 的诱发因素之一 (11)。此外，使用广谱抗菌药物会提高活动期 IBD 患者发生艰难梭菌感染的风险，这是 IBD 患者最常见的感染性并发症之一，并会进一步增加需要结肠切除术的风险 (12)。因此，开发可替代抗生素的治疗手段成为重要研究方向。

多项研究表明，通过靶向调控肠道细菌生物膜可缓解小鼠实验性结肠炎 (13, 14)。季铵盐（QAS）是一类阳离子化合物，当铵离子的四个氢原子被烃基取代后形成。QAS 是常见的杀菌成分，其可吸附于细胞表面，疏水基团插入脂质层，使细胞膜通透性增加并被破坏，从而干扰细胞代谢并导致真菌或细菌死亡。此外，QAS 还可干扰核酸和蛋白质合成 (15)。因此，我们推测 QAS 可以通过清除肠道细菌生物膜来改善 UC。

JUC 喷雾敷料（其在美国 FDA 和欧盟 CE 认证中的名称；中国医疗器械名称为“长效抗菌材料”）是一种新型有机硅双长链二季铵盐制剂，利用硅材料的高疏水性改善了化合物的水溶性。当 JUC 喷雾敷料接触皮肤或黏膜表面时，会形成双层抗菌结构，包括黏附层和带正电荷层。黏附层确保材料能牢固附着于表面，而带正电荷的季铵盐可通过静电作用破坏带负电的细胞壁和细胞膜，从而发挥杀菌作用。既往研究表明，JUC 喷雾敷料能够通过物理方式杀灭多种细菌以抑制其生长 (16)。目前该产品已广泛用于创面治疗和留置器械护理。尽管已有研究证明 JUC 喷雾敷料对人体安全无毒，但其对肠道细菌的杀菌作用仍缺乏研究证据 (17)。

因此，本研究旨在评估 JUC 喷雾敷料在 DSS 诱导的 UC 小鼠模型中的治疗效果。同时，我们通过电镜观察生物膜、评估肠屏障功能、分析微生物群结构来探讨其潜在作用机制。

鉴于溃疡性结肠炎涉及黏膜生物膜形成，本研究选择采用结肠局部给药方式，以验证 JUC 喷雾敷料作为“生物膜靶向制剂”的作用。该方法旨在最大限度清除病灶部位的局部生物膜，同时减少全身暴露。然而，目前尚未明确 JUC 在胃肠道黏膜环境中的药代动力学和腔内滞留情况，仍需进一步的专门研究。

2 方法

2.1 试剂

DSS（分子量 36,000 – 50,000 Da）购自 MP Biomedicals（美国加州圣安娜）。粪便潜血检测试剂盒购自南京建成生物工程研究所（中国南京）。小鼠白细胞介素-6（IL-6）、白细胞介素-1β（IL-1β）和肿瘤坏死因子-α（TNF-α）ELISA 试剂盒购自 R&D Systems（美国明尼苏达州明尼阿波利斯）。水合氯醛溶液购自 Legend Biotech（中国北京）。甲硝唑（MTZ，0.5 g/100 mL）由石家庄四药有限公司（中国石家庄）提供；美沙拉嗪（28 g/60 mL）购自 Dr. Falk Pharma GmbH（德国弗赖堡）。JUC 喷雾敷料购自南京纳迈斯科技有限公司（中国南京）。

2.2 动物实验设计

由于本研究为 JUC 喷雾敷料的首次体内评价，因此选用较小样本量，旨在获得初步数据，为后续更复杂的实验研究提供依据。6–8 周龄、体重 20–24 g 的雄性 C57BL/6J 小鼠（n = 50）购自 Charles River（中国浙江）。小鼠饲养于恒温恒湿环境（20 ± 2° C，湿度 45 ± 5%，12 小时光/暗周期），每笼 5 只，可自由摄取标准饲料。

适应性饲养 1 周后，将小鼠随机分为 5 组（每组 n = 10）：

1）正常对照组；

2）DSS + PBS 组；

3）DSS + JUC 组；

4）DSS + 甲硝唑（DSS + MTZ）组；

5）DSS + 美沙拉嗪（DSS + 5-ASA）组。

每个处理组的 10 只小鼠饲养于 2 个笼位中。随机分组使用 Microsoft Excel 2021 中的 RAND() 函数完成。

UC 模型的建立方法依据文献 (18)。简而言之，给予 3%(w/v)新鲜 DSS 自由饮用 7 天以诱导急性 UC；正常组饮用无菌水。第 7 天开始给予灌肠（200 mM/只，0.008 mL/g/天），不同组分别给予 PBS、JUC、MTZ（1 g/L）或 5-ASA（19, 20）。灌肠前禁食 12 小时，并经腹腔注射 10%（v/v）水合氯醛（50 mM/只）麻醉，5–10 分钟起效。灌肠时间均安排在治疗日的 12:30–14:30，通过随机顺序避免昼夜节律或操作人员偏倚。所有操作过程在组间保持一致。

灌肠后小鼠尾部倒悬 2 分钟，再返回原笼。实验期间每日观察并记录体重、粪便潜血、腹泻和粪便性状，并计算疾病活动指数（DAI）。测试时间为每日 12:30–14:30，测试顺序每日随机，每只动物在不同日接受不同时间的测试。若小鼠体重低于 15 g，则需实施安乐死。

实验第 12 天，小鼠被处死，取肛门上方 1 cm 的结肠段，并用 4%（w/v）多聚甲醛固定用于后续实验。麻醉使用腹腔注射 350 mg/kg 水合氯醛，可维持约 2 小时轻度麻醉，肌松作用有限；高剂量可抑制心肌收缩并引起心律失常，因此全过程密切监测。实验中未发生与操作相关的穿孔或早死。其余结肠组织储存于 -80° C。

所有小鼠的评分由三名不同研究者完成，其中两名对处理组盲法。若灌肠成功则纳入研究；若灌肠插入导致穿孔或动物提前死亡，无法获得行为学或组织学数据，则排除。所有评价均采用盲法完成，三名实验者评分一致性较高（κ > 0.8），分歧通过讨论解决。本研究中无小鼠发生穿孔或早死，因此无因操作问题被排除的动物。

2.3 炎症评估

通过体重变化、DAI、结肠长度及组织学评分评估 UC 模型的建立情况及治疗效果。所有收集的数据均纳入统计分析。

DAI 评分标准如下：

1）体重变化：0：<1%；1：1–5%；2：5–10%；4：>15%；

2）粪便性状：0：正常；2：稀软；4：腹泻；

3）粪便带血：0：阴性；2：阳性；4：肉眼可见出血。

4% 多聚甲醛固定的结肠组织经石蜡包埋、切片、苏木精–伊红染色（H&E）。根据隐窝损伤、溃疡及中性粒细胞浸润情况进行评分，具体标准如下：

1）炎症程度：0：无；1：轻度；2：中度；3：重度；

2）炎症范围：0：无；1：黏膜层；2：黏膜及黏膜下层；3：全层；

3）隐窝损伤程度：0：无；1：基底 1/3 损伤；2：基底 2/3 损伤；3：仅表层上皮完整；4：隐窝与上皮完全丧失；

4）浸润面积百分比：1：1–25%；2：25–50%；3：51–75%；4：76–100%。

每张组织切片随机选择 3 个以上高倍视野（×400），由两名盲法研究者评分，取平均值作为最终结果。

2.4 免疫组织化学与免疫荧光

组织切片先使用非特异性封闭试剂封闭背景染色，然后孵育相应的一抗及 HRP 标记的二抗。使用 Nikon E100 光学显微镜

（Nikon，日本东京）获取图像。每个样本随机选择至少三个视野，在 40× 物镜下成像，并使用 ImageJ 软件进行半定量蛋白表达分析。蛋白表达强度以阳性信号所占面积表示。

结肠中紧密连接（TJ）相关蛋白的表达通过免疫荧光检测。图像使用 Nikon ECLIPSE TI-SR 荧光显微镜获取。IHC 染色采用 H-score / 平均光密度进行定量；免疫荧光指标（MUC2、ZO-1、Occludin）则测量平均荧光强度。设置阴性对照（省略一抗）及同型对照以验证染色特异性。

2.5 杯状细胞计数

石蜡包埋结肠组织切片经脱蜡、水化后浸入蒸馏水，再放入高碘酸溶液中，于室温孵育 1.5 小时；随后浸入蒸馏水，过 Schiff 试剂染色，于 37° C 烘箱脱水 20 分钟，再用蒸馏水冲洗 10 分钟，分级脱水，经二甲苯透明后用中性树胶封片。染色后，结肠杯状细胞呈深蓝色，周围组织呈浅蓝或无色。切片分析使用 Image-Pro Plus 6.0 软件进行。

2.6 电镜观察

每组随机选择 3 只小鼠的肠黏膜进行电镜观察。取距肛门 1 cm 的结肠组织并固定于 2.5% 戊二醛中。每份标本选取 3 个视野进行观察。肠黏膜表面生物膜采用 SU8100 扫描电镜（SEM；Hitachi，日本东京）观察；上皮细胞间紧密连接则使用 HT7700 透射电镜（TEM；Hitachi）观察。

2.7 血清细胞因子 ELISA 分析

使用 R&D Systems 公司提供的特异性 ELISA 试剂盒，按照说明书检测血清促炎性细胞因子水平。

2.8 16S rRNA 扩增子测序分析

使用 Mag Pure Soil DNA KF Kit（安戈生物，中国广州）从小鼠盲肠内容物中提取基因组 DNA，并通过琼脂糖凝胶电泳检测其纯度和浓度。以稀释后的基因组 DNA 作为模板，使用针对细菌 16S rDNA（V3–V4）区域的引物

前向引物：343F（5′-TACGGRAGGCAGCAG-3′）
反向引物：798R（5′-AGGGTATCTAATCCT-3′）
进行 PCR 扩增和纯化。

根据序列比对结果，利用 PyNAST 软件构建操作分类单元（OTUs）的代表序列系统发育树。对测序数据进行预处理后，获得高质量序列，并根据相似性聚类为多个 OTUs。随后分析微生物群的 α 多样性、β 多样性、分类学组成及菌群结构，并进行 16S 功能基因预测。

2.9 统计学分析

使用 GraphPad Prism（GraphPad Software，美国加州拉霍亚）进行统计分析与图表绘制。采用 Kolmogorov–Smirnov 方法检验数据分布；$P > 0.1$ 认为符合正态分布。组间均值比较使用单因素方差分析（One-way ANOVA），随后进行 Tukey 事后检验。$P < 0.05$ 表示差异具有统计学意义。

3 结果

3.1 JUC 喷雾敷料改善 DSS 诱导的结肠炎

在 DSS 诱导的结肠炎期间，小鼠逐渐出现体重下降、腹泻及便血等症状。与正常对照组相比，DSS+PBS 组小鼠体重显著下降，DAI 明显升高。灌肠治疗后，三种药物治疗组的体重下降症状均有所改善，且 DAI 显著降低（$P < 0.01$）。但三组之间差异均无统计学意义（$P > 0.05$）（图 1A、1B）。

这些结果表明 JUC 喷雾敷料可减轻 UC 小鼠的体重下降及活动度降低，与 MTZ 或 5-ASA 的治疗效果相当。

在图 1A 和图 1B 的时间进程分析中，DSS+JUC 组与 DSS+PBS 组相比无统计学差异（P > 0.05）。JUC、MTZ 与 5-ASA 之间的比较亦未达到统计学差异。

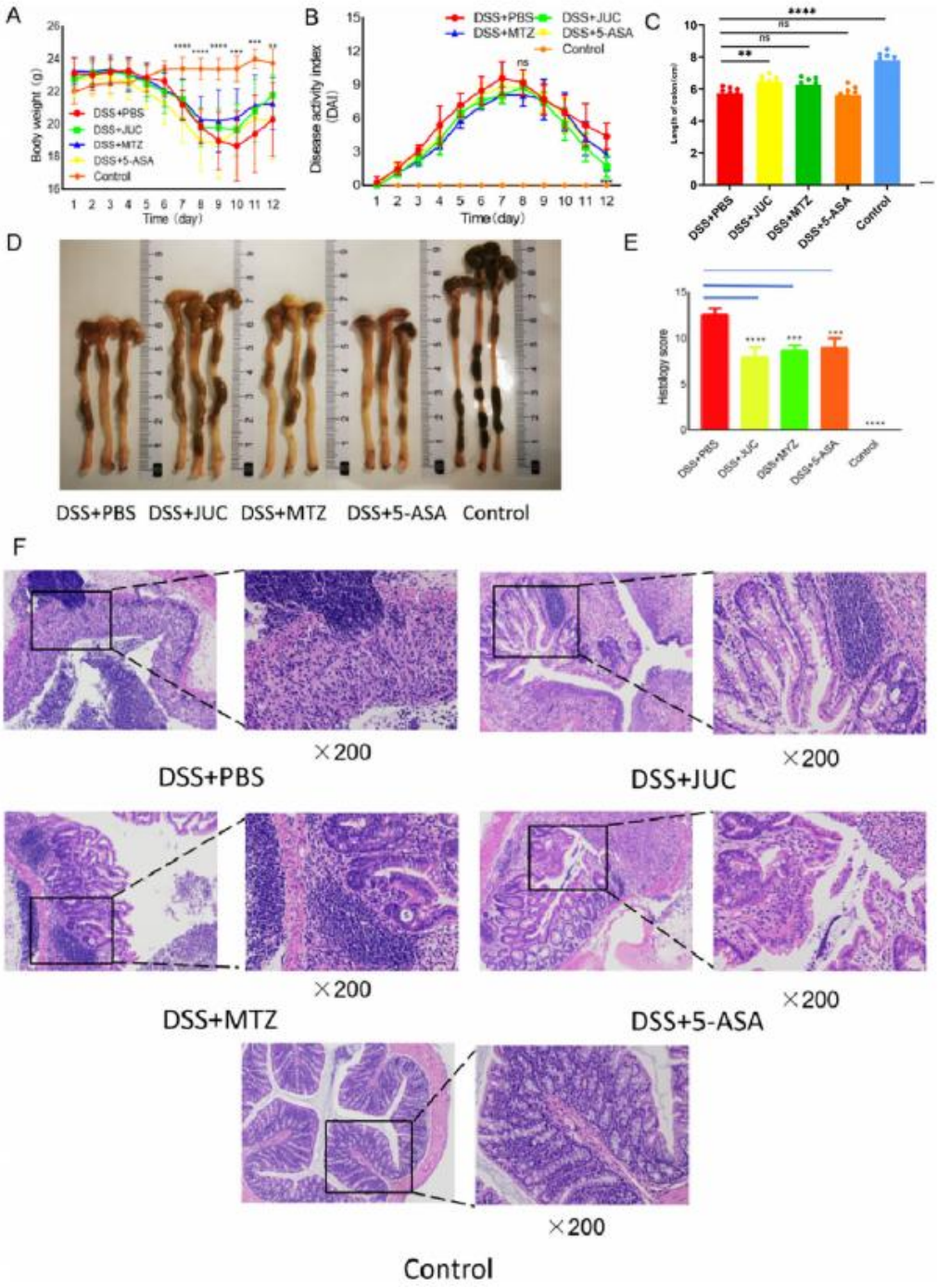

JUC 喷雾敷料对小鼠肠道炎症的影响。

(A) 小鼠体重变化（N = 10），**P<0.01，***P<0.001，****P<0.0001，与 DSS+PBS 组相比。

(B) DAI 评分变化（N = 10，***P<0.001，与 DSS+PBS 组相比）。

(C) 结肠长度比较（N = 10，*P<0.05，****P<0.0001，与 DSS+PBS 组相比）。

(D) 小鼠结肠的宏观外观。

(E) 小鼠结肠组织的组织学评分，***P<0.001，****P<0.0001，与 DSS+PBS 组相比。

(F) 药物对小鼠结肠病理性改变的影响（HE×200）。

统计学分析：

连续性多组比较（例如小鼠体重、图 1A；结肠长度、图 1C）采用 Tukey 事后多重比较检验（HSD），用于严格评估组间均值的两两差异。

顺序/评分类结局指标（如疾病活动指数 DAI、图 1B；组织学评分、图 1E）在数据近似满足正态性和方差齐性时采用 Student t 检验；若不满足，则采用非参数 Mann–Whitney U 检验。

双侧检验，$P < 0.05$ 被视为具有统计学显著性。

DSS+PBS 组小鼠出现明显的结肠痉挛，其肠内容物不成形。实验结果见图 1C、1D。与正常对照组相比，DSS+PBS 组的结肠出现肿胀、充血，并伴有明显的痉挛缩短（$P < 0.0001$）。DSS+JUC 组小鼠的结肠长度较 DSS+PBS 组显著增加（$P < 0.05$）。三种治疗均能有效缓解 UC 小鼠的结肠痉挛。

组织病理学是评价结肠健康的重要依据。如图 1E、1F 所示，正常对照组小鼠的结肠黏膜完整、腺体排列整齐，无炎性水肿。在 DSS+PBS 组中，结肠组织损伤严重，肠黏膜出现脱落和坏死，可见典型隐窝脓肿，同时伴随腺体缺失、部分隐窝损伤、杯状细胞减少、大量炎性细胞浸润及全层炎症。JUC 喷雾敷料、MTZ 与 5-ASA 灌肠治疗均可减轻炎性细胞浸润，减少病灶深度和范围，从而显著降低组织学评分（$P < 0.001$）。

3.2 JUC 喷雾敷料减少结肠细菌生物膜

我们对 SEM 图像进行了定量分析，使用 ImageJ 计算各组肠黏膜表面被生物膜覆盖的比例，并采用单因素方差分析结合 post hoc 检验比较组间差异（图 2B）。在统一放大倍率与随机视野选取条件下，JUC 组的生物膜覆盖率显著低于 DSS+PBS 组。

扫描电子显微镜（SEM）用于评估 JUC 喷雾敷料对肠道细菌生物膜的影响。DSS+PBS 组在所有 9/9 的图像中均可观察到明显生物膜结构。

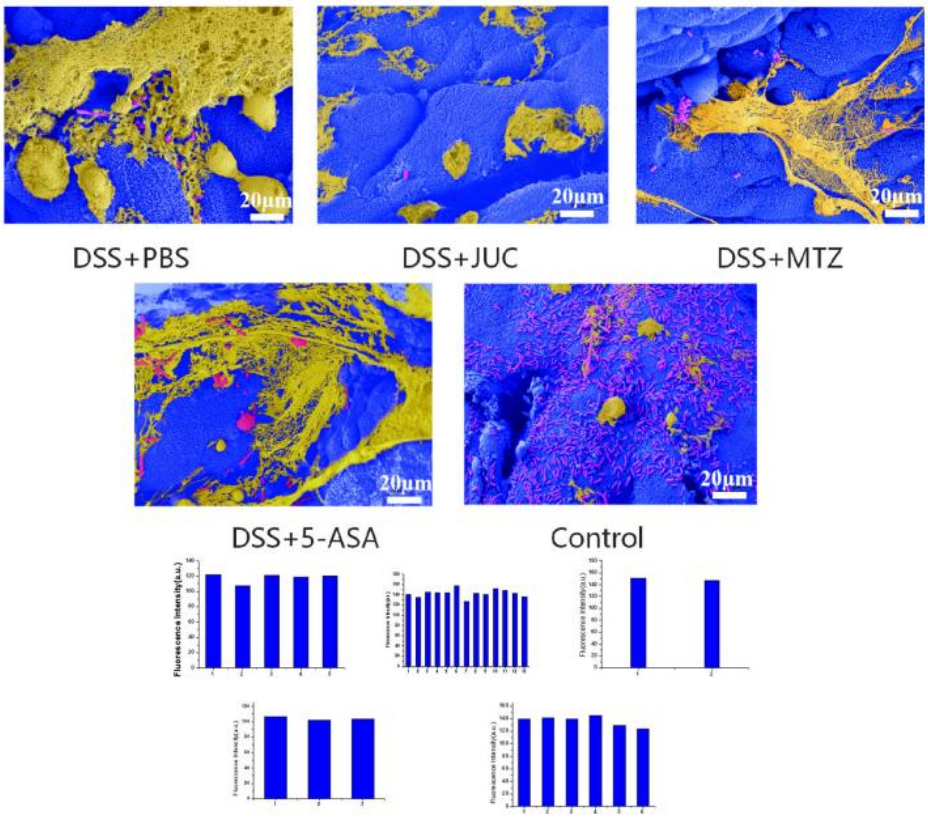

图 2. 肠黏膜表面的细菌生物膜，经扫描电镜（1000×）观察。

通过 SEM 图像对生物膜覆盖面积进行定量分析。生物膜面积使用 ImageJ 测量，并以黏膜表面被附着生物膜覆盖的百分比表示。柱状图显示动物间的平均值 ± 标准差（mean ± SD）；所有视野均在相同放大倍率下随机选取。统计分析采用单因素方差分析（One-way ANOVA）及 Tukey 事后检验。星号表示与 DSS+PBS 组相比具有显著性差异（$P < 0.05$，*$P < 0.01$，**$P < 0.001$）；括号明确标示比较的组别。

相较之下，DSS+JUC 组中 8/9 张图像、DSS+MTZ 组中 6/9 张图像显示生物膜覆盖显著减少。而在正常对照组中，肠黏膜表面的细菌多以悬浮（planktonic）状态存在。如图 2 所示，UC 模型小鼠的结肠中广泛存在生物膜，并被厚实基质覆盖。除结构多样的细菌外，还可观察到大量水道结构（water channels）。不同于 UC 模型组，正常对照组结肠黏膜中的细菌多以游离形式存在，生物膜形成较少。

MTZ 和 5-ASA 的治疗使 EPS 基质变薄，暴露出细菌本体；而 JUC 喷雾敷料治疗则显著减少生物膜形成。

SEM 定量分析（图 2B）显示，与 DSS+PBS 组相比，DSS+JUC 组肠黏膜表面的生物膜覆盖率显著降低，并与观察到的胞外聚合物（EPS）基质的可见变薄以及细菌暴露程度一致。从生物学角度来看，表面生物膜结构减少预计可降低上皮 PRR（如 TLR2/4）的激活，并减少下游 NF-κB 信号通路的激活，这与本研究中观察到的 IL-6、TNF-α、IL-1β 的降低以及紧密连接形态与 IF 标志物（MUC2、ZO-1、occludin）的改善趋势一致。

3.3 JUC 喷雾敷料降低炎性细胞因子水平

与 UC 密切相关的主要促炎细胞因子包括 IL-6、IL-1β 和 TNF-α (21)。本研究通过 ELISA 检测血清中炎症因子水平，并结合结肠末端组织的免疫组化结果进行评估，如图 3 所示。

在 DSS+PBS 组中，IL-6、IL-1β 和 TNF-α 的水平均显著高于正常对照组（$P < 0.0001$）。经 JUC 喷雾敷料、MTZ 或 5-ASA 治疗后，IL-6 显著下降（$P < 0.0001$），TNF-α（$P < 0.0001$）和 IL-1β（$P < 0.001$）亦呈显著降低。三种治疗方案之间的差异无统计学意义（$P > 0.05$）。

定量免疫组化分析显示，与血清 ELISA 的结果趋势一致，各治疗组均出现 IL-6、IL-1β 和 TNF-α 的降低，提示结肠组织炎症水平与血清检测具有一致性。

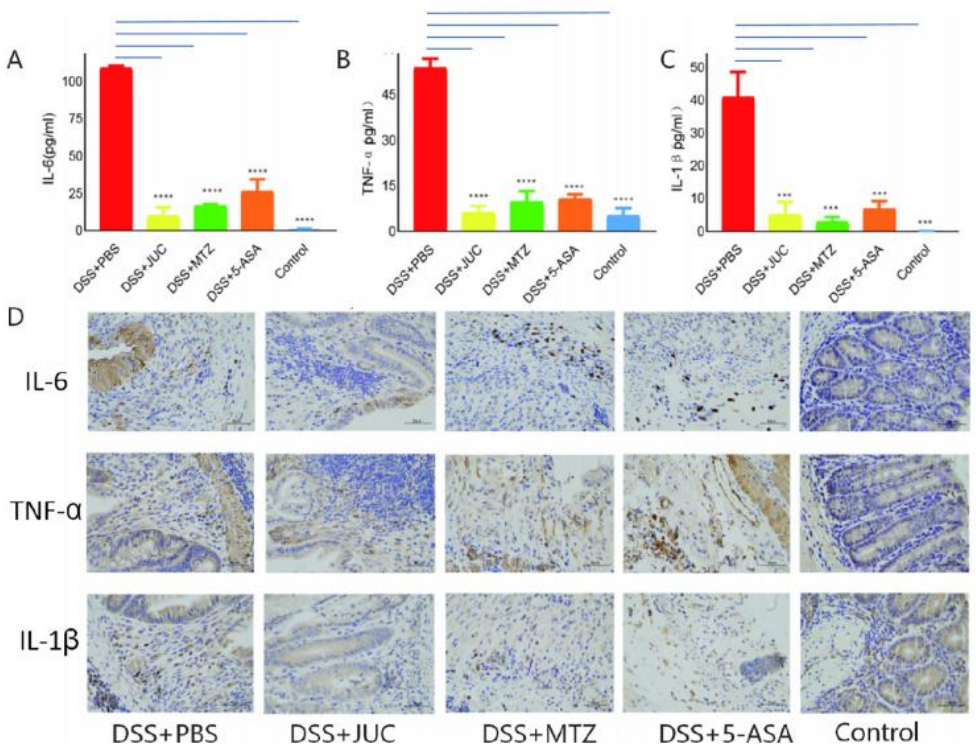

图 3. JUC 喷雾敷料对外周血炎性因子水平的影响。

(A) IL-6 的表达（N = 3）。

(B) TNF-α 的表达（N = 3）。

(C) IL-1β 的表达（N = 3）。

P < 0.001，*P < 0.0001，与 DSS+PBS 组比较。

(D) 末端结肠（200×）炎症因子的免疫组化分析。

统计分析：血清炎性细胞因子（TNF-α、IL-6、IL-1β）的多组连续比较采用 Tukey's HSD（Honestly Significant Difference）检验，并进行多重比较校正以评估组间两两差异。双侧检验 P < 0.05 视为具有统计学意义。

3.4 JUC 喷雾敷料改善肠屏障功能

DSS 诱导 UC 后，TEM 显示上皮细胞间连接异常，包括紧密连接（tight junction, TJ）复合体的分离和旁细胞间隙（paracellular spaces）扩大。在 DSS+PBS 组中，黏液层同样受损，在显微镜下变薄，顶端结构肿胀、脱落，细胞排列紊乱，细胞器出现肿胀及坏死。相比之下，正常对照组的肠黏膜绒毛结构规则、排列紧密，器官结构完整、细胞间连接良好。

JUC、MTZ 和 5-ASA 处理均可改善异常的紧密连接结构和细胞质形态（cytodedema），并缓解炎症导致的屏障结构松散（图 4A）。黏蛋白 2（MUC2）是由杯状细胞分泌的高分子量糖蛋白，是肠腔内重要的黏液屏障 (8)。在 DSS 诱导 UC 后，肠屏障受损（图 4B），杯状细胞数量减少（图 4C）。TJ 蛋白是维护屏障完整性、阻止肠腔内容物渗漏的重要结构 (8)。免疫荧光数据显示，在 DSS+PBS 组中，ZO-1 和 Occludin 表达减少，肠屏障结构松散（图 4D）。

JUC、MTZ 和 5-ASA 治疗均改善了 TJ 蛋白表达，其中 JUC 和 5-ASA 组 MUC2 表达增加，而 MTZ 组 MUC2 表达未显著变化。免疫荧光定量结果显示，与 DSS+PBS 组相比，所有治疗组 ZO-1 和 Occludin 表达均显著升高；MUC2 在 JUC 和 5-ASA 组增加，在 MTZ 组不显著（图 4E）。

3.5 JUC 喷雾敷料改善肠道微生物组成

我们通过 16S rRNA 测序分析盲肠内容物的 α 多样性与 β 多样性。与 DSS+PBS 组相比，JUC 显著提高 α 多样性，并改变 β 多样性，而门水平（phylum-level）的优势菌群组成未发生显著变化（图 5）。该模式提示 JUC 促进微生物群落的均衡恢复（evenness），而非导致广泛菌群消耗（broad depletion）。这一结果与 JUC 的选择性生物膜靶向作用相符，意味着其主要通过减少生物膜相关致病菌、降低炎症，而不是通过大范围清除肠道菌群达到效果。

需要注意的是，本研究取样来源为盲肠内容物，而非肠黏膜附着菌群（mucosa-associated communities），后者可能低估生物膜相关菌群（biofilm-resident taxa）的比例。未来研究将取黏膜刮片或活检样本，并结合 FISH 等技术直接评估生物膜相关菌群。

为了评估 JUC 对肠道菌群的影响，我们对 DSS 处理后的小鼠进行 16S 测序，每组 6 只动物纳入 OTU 分析。OTU 维恩图显示，共鉴定到 926 个 OTUs，包括 DSS+PBS、DSS+JUC、DSS+MTZ、DSS+5-ASA 及正常对照组共有及独有的 OTUs（图 5A）。

β 多样性分析用于比较不同组间的群落结构差异。基于主坐标分析（PCoA）和热图（heatmap），可见 DSS+PBS 组的菌群结构明显偏离正常对照组，而 JUC、MTZ 和 5-ASA 处理后 β 多样性均有所恢复（图 5B）。α 多样性小提琴图显示 DSS+PBS 组物种丰富度和分布度最低，而 JUC 和 MTZ 处理显著提高了 α 多样性（$P < 0.05$）。DSS+5-ASA 组与 DSS+PBS 组相比无显著差异（图 5C）。

菌群构成直方图（图 5D）显示 DSS+PBS 组拟杆菌门（Clostridium spp.）比例增加，而治疗组该比例降低。

门水平分析未显示 DSS+JUC 与 DSS+PBS 之间的显著差异，但 α、β 多样性均显示 JUC 可改善菌群结构。

热图进一步显示，健康组中 Roseburia 与 Butyricimonas 等益生菌更为丰富；DSS+PBS 组益生菌相对减少，而 Bacteroides、Dorea 及部分厌氧菌（anaerobic bacteria）比例增加。JUC 处理则逆转了该趋势，降低潜在有害菌（如 Bacteroides spp.）比例，同时维持整体菌群结构的稳定性（图 5E）。

综上，JUC 具有选择性的生物膜靶向作用，可减少潜在有害菌并改善菌群均衡，而不会导致整体微生物群的大规模丢失，呈现比广谱抗菌策略更理想的生态稳定性。

4 讨论

本研究采用 DSS 诱导的小鼠溃疡性结肠炎模型来评估 JUC 喷雾敷料的治疗效果(23)。在连续 7 天给予 DSS 后，小鼠出现活动能力显著下降、体重减轻、脓性腹泻和便血等症状。血清中炎性因子水平升高，结肠腺体结构紊乱、肠黏膜脱落与坏死、大量炎性细胞浸润，以及典型隐窝脓肿的形成，均表明该模型成功诱导了小鼠肠炎，能够有效模拟临床 UC 的病程 (24)。

除了整体性的 PRR－NF-κB 信号通路的抑制外，菌种特异性的微生物相互作用以及特定细胞靶点（如巨噬细胞亚群、Th17 细胞）也值得进一步研究，以深入阐明其分子机制。许多细菌含有胞内多磷酸，可使细菌更易受到氧化应激，进而降低定植与生物膜形成能力 (25)。本研究的结果证实，5-ASA 对结肠生物膜具有一定的清除作用，同时可改善小鼠肠炎。目前尚无研究报道 QAS（季铵盐）、COX 和 PGI 之间的直接关系，这表明 QAS 改善炎症的机制仍需进一步探索。

有学者提出，在 IBD 患者中，窄谱抗生素往往无法达到广谱抗生素的治疗效果，这提示减少结肠细菌负荷可能比广泛杀菌更能有效控制 IBD 的疾病活动度 (26, 27)。本研究结果支持这一观点：无论是广谱抗菌剂还是 JUC 喷雾敷料的物理杀菌方式，都可以通过降低结肠的细菌负荷来改善实验性结肠炎。

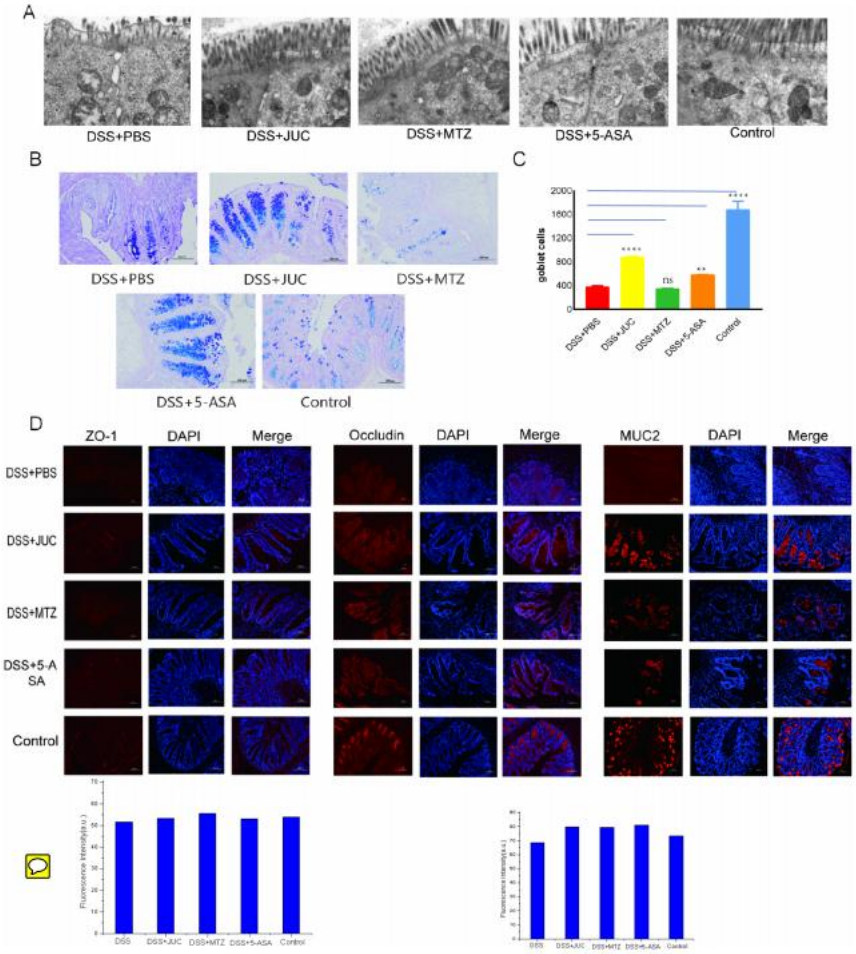

图 4. JUC 喷雾敷料对肠屏障功能的影响。

(A) 肠道机械屏障，由透射电镜观察。

(B) 远端结肠的过碘酸-Schiff（PAS）-阿利新蓝（AB）染色（200×）。

(C) 杯状细胞计数。

(D) 上皮屏障标志物的免疫荧光分析（MUC2、ZO-1、Occludin，200×）。

(E) 上皮屏障蛋白（MUC2、ZO-1、Occludin）免疫荧光定量。信号强度以 ImageJ 测量的平均荧光强度表示。

柱状图显示动物间的平均值 ± 标准差（mean ± SD）；所有视野在相同成像设置下随机选取。统计学分析采用单因素方差分析（One-way ANOVA）并结合 Tukey’s post hoc 检验。星号表示与 DSS+PBS 组相比具有显著性差异（$P < 0.05$，*$P < 0.01$，**$P < 0.001$）；括号明确标示比较的组别。

显微图像使用 ImageJ 进行自动细胞计数；细胞数量根据特定标志物的免疫荧光阳性信号确定。连续多组比较使用 Tukey’s Honestly Significant Difference（HSD）检验，并进行多重比较校正以评估组间两两差异。双侧检验 $P < 0.05$ 视为具有统计学意义。

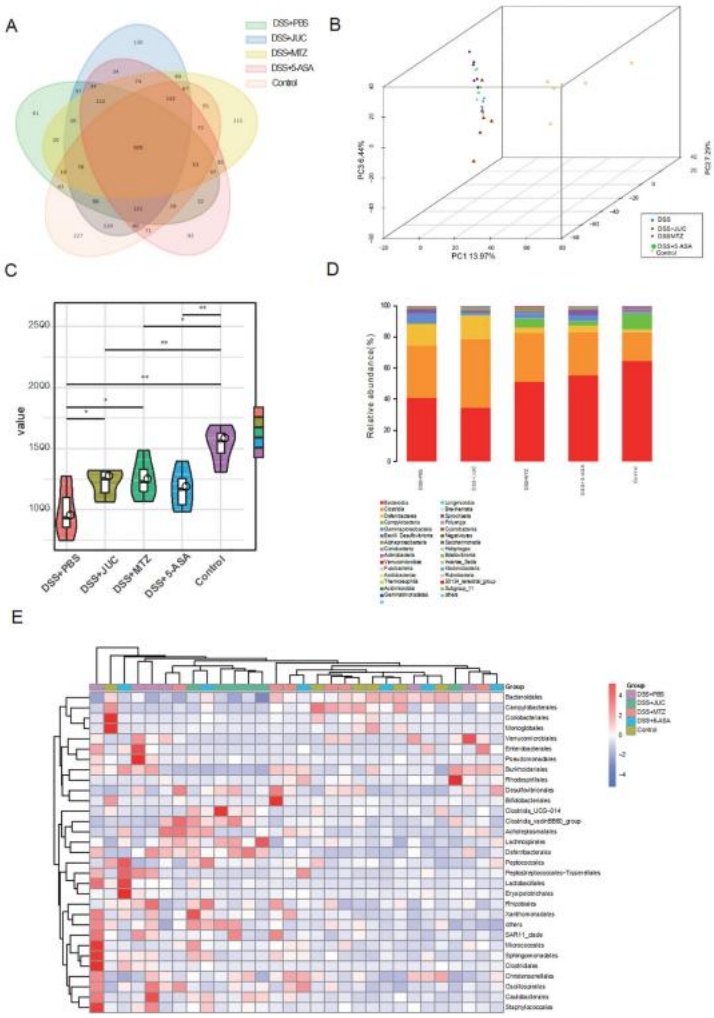

图 5. 肠道菌群变化。

(A) OTU 维恩图。

(B) β 多样性分析。

(C) α 多样性分析。

*P < 0.05，**P < 0.01，与 DSS+PBS 组比较。

(D) 菌群组成直方图。

(E) 菌群结构热图。

机制层面分析

生物膜的清除可减少上皮组织中模式识别受体（PRR），特别是 TLR2/TLR4 的激活，从而下调 NF-κB 信号通路，减少 IL-6、TNF-α、IL-1β 等炎性因子产生。此外，TLR/NF-κB 信号的削弱可能改变巨噬细胞亚群并抑制 Th17 反应。这些假设仍需通过精确模型（如无菌动物模型或上皮/免疫细胞共培养系统）进一步验证，以阐明其分子机制及特异性。

本研究中的三种治疗方案均显著降低了 DSS 诱导性结肠炎中炎症细胞因子的表达，表明它们均具有减轻实验性结肠炎的能力。5-ASA 的作用靶点与非甾体抗炎药（NSAIDs）类似，通过抑制环氧合酶（COX）和前列腺素（PGI）的产生来减少肠道炎症和细胞增殖，并促进凋亡。因此，5-ASA 已被广泛用于改善肠道炎症和预防肿瘤发生 (41)。Dahl 等研究者报道，5-ASA 可降低许多细菌的多磷酸盐水平，使细菌更易受到氧化应激，进而减少定植和生物膜形成。

生物膜与肠道屏障损伤的关系

先前研究推测 IBD 可能是一种与微生物相关的疾病 (38)。大型细菌群落形成的生物膜可增强细菌穿透能力，破坏黏液屏障，使细菌直接接触肠上皮细胞，引发异常的免疫反应，进一步促进疾病的发展与迁延 (39)。另一项研究表明，在 IBD 患者的肠黏膜活检标本中比健康人更易观察到生物膜 (13)。与此一致，本研究的扫描电镜结果显示，DSS+PBS 组的结肠黏膜存在数量更多、结构更复杂的生物膜。生物膜中可见多种细菌参与物质交换和营养互作，部分益生菌也可能参与其中 (6)。相反，正常对照组黏膜上的细菌多以浮游状态存在。

MTZ 与 5-ASA 使生物膜基质变薄并暴露细菌，而 JUC 则显著减少了生物膜的形成与细菌丰度，并在较大范围内破坏 EPS 基质结构，提示 JUC 对生物膜具有强效清除作用。

JUC 的选择性杀菌与肠道菌群稳定性

由于 JUC 为物理杀菌方式，它不依赖特定代谢通路，不易诱导细菌耐药。已有研究报道 JUC 对多种微生物均有效，其在皮肤和导尿管护理中被广泛应用，并且安全无毒 (16, 17)。本研究结果进一步支持其可通过减少结肠生物膜而改善小鼠结肠炎。

IBD 患者存在肠道屏障功能障碍与菌群失调 (28)。肠黏膜生物膜在 IBD 患者中更为常见，并与更高程度的炎症密切相关 (31, 32)。生物膜可导致局部细胞抗原、毒素与有害代谢物堆积 (33)，进一步破坏屏障，使细菌入侵肠上皮 (34)。因此，靶向生物膜形成已成为 IBD 新兴的治疗策略之一。

本研究显示，DSS+PBS 模型组的小鼠肠道菌群紊乱，α 与 β 多样性明显降低；而 JUC 组显著改善了菌群多样性，其改善程度与 MTZ 和 5-ASA 组相似，且未表现出对肠道菌群组成的广泛破坏。

这表明 JUC 在杀灭潜在有害菌（如 Bacteroides spp.）的同时，仍可维持整体微生物群结构的生态稳定性。

例如，柠檬酸类两性表面活性剂可螯合 EPS 中的钙离子桥，使生物膜结构变得松散，更易被破坏 (42)。此外，蛋白酶还可促进生物膜的消化。IBD 患者通常具有更大、更致密的黏膜生物膜，菌体浓度高于健康人；然而，氢溴酸盐类衍生物能够去除这些结构。Mota 等人报道，直接降低微生物黏附能力可减少 IBD 相关生物膜形成，而不会显著改变菌群组成，从而改善硫嘌呤类药物诱导的结肠炎 (13)。

本研究结果同样显示，JUC 喷雾敷料可减少生物膜形成，而不显著改变菌群结构。然而，与前述利用金属螯合剂破坏 EPS 基质的研究不同，JUC 喷雾敷料通过电静力作用杀灭细菌，从而破坏细菌生物膜。在与抗生素联合应用时，JUC 可能增强抗生素穿透生物膜的能力，使其在未来具有潜在应用价值。目前尚无明显毒性报道，但仍需药代动力学研究以确认其安全性与局部暴露情况。因此，本研究仅提供安全性趋势推断，未来需进一步量化局部浓度、滞留时间及黏膜渗透性，并辅以毒理研究。

既往研究表明，生物膜可能与多种疾病相关，如食管炎、腺瘤性息肉和结直肠癌 (43, 44)。未来研究需探讨生物膜是否参与这些疾病的进展。此外，尽管小鼠常用于肠道菌群研究，但其盲肠占体积比例远高于人类，因此某些现象在人类中的可比性需进一步验证 (45, 46)。电镜观察虽然可用于可视化生物膜，但无法直接量化生物膜的厚度与密度；未来应结合三维成像或 in situ 荧光杂交（FISH）等技术以获得更精准的生物膜信息。

长期意义

尽管 JUC 具有杀菌作用并可能增加益生菌（如 Roseburia、Butyricimonas）等比例，但其 α 和 β 多样性改善仅伴随轻微的门水平变化，没有导致广泛的菌群重构。这说明 JUC 可通过选择性破坏生物膜来减少炎症诱导因素，同时维持菌群整体稳定性。相比之下，MTZ 导致更广泛的菌群扰动，而 5-ASA 虽具有抗炎作用，但不直接靶向生物膜。

因此，从长期来看，JUC 的优势可能来自于：减少有害生物膜相关刺激，而非广泛杀菌；维持菌群生态稳定，避免显著失衡；

通过改善屏障功能与降低炎症设定点来促进黏膜修复。
本研究仍有若干局限：
1）样本量较小，可能无法检测更细微的组间差异，需在后续研究中增加样本量；
2）未进行直接的屏障通透性检测（如 FITC-dextran 试验）；
3）生物膜定量仅依赖图像分析，需要标准化的自动化流程以提高可重复性。
展望：
由于 DSS 主要导致急性结肠炎，未来应采用慢性或复发性模型以及功能性指标（如短链脂肪酸代谢、黏液层完整性）以验证 JUC 在长期疾病控制中的价值。

5 结论

本研究评估了一种有机硅双长链二季铵盐制剂（Organosilicone Double-Long-Chain Diquaternary Ammonium Salt），以 JUC 喷雾敷料为代表，在 DSS 诱导的小鼠结肠炎模型中的治疗作用，并将其与 MTZ 和 5-ASA 等常规治疗进行比较。
研究结果显示，JUC 的治疗效果与传统药物相当，提示其可能成为溃疡性结肠炎的一种替代治疗选择，但仍需更大规模的研究进一步验证其可比性。
本研究的发现进一步支持以下假设：
1）微生物感染（特别是生物膜相关病原体）可能参与 UC 的发病机制；
2）控制细菌生物膜形成可减轻肠道炎症。
这些结果为有机硅双长链二季铵盐在 UC 管理中的潜在临床应用提供了重要的研究线索。

数据可得性声明

本研究中呈现的原始数据已包含于文章和补充材料中。更多信息可向通讯作者索取。

伦理声明

本动物研究经东部战区总医院动物伦理委员会批准。所有实验均按照当地法律法规和机构要求开展。

作者贡献

SS：撰写——初稿。
GT：撰写——初稿。
JW：撰写——审阅与编辑。
SS：撰写——审阅与编辑。
ZD：撰写——审阅与编辑。
QA：撰写——审阅与编辑。
HT：撰写——审阅与编辑。
FW：撰写——审阅与编辑。

经费支持

作者声明，本研究的研究和/或发表工作获得资金支持。本研究得到国家自然科学基金资助（No. 81873559；No. 82170574）。

致谢

我们感谢汪芳裕教授的悉心指导和帮助。感谢南京神奇科技开发有限公司提供技术支持。

利益冲突声明

作者声明，在本研究的进行过程中不存在任何可能被视为潜在利益冲突的商业或经济关系。

生成式人工智能声明

作者声明，本手稿的撰写过程中未使用任何生成式人工智能工具。
文中用于图像的替代文本（alt text）由 Frontiers 在人工智能技术支持下生成，并经作者在可能情况下进行准确性审阅。如您发现任何问题，请联系我们。

出版者声明

本文中的所有观点仅代表作者个人观点，不

一定代表其所属机构、出版社、编辑或审稿人的立场。文中涉及的任何产品评价或制造商声明，均不代表出版者的保证或认可。

参考文献

1. Fodil N, Moradin N, Leung V, et al. CCDC88Bis required for pathogenesis of inflammatory bowel disease. *Nat Commun.* (2017) 8:932. doi: 10.1038/s41467-017-01381-y

2. Rubin SJS, Bai L, Haileselassie Y, et al. Mass cytometry reveals systemic and local immune signatures that distinguish inflammatory bowel diseases. *Nat Commun.* (2019) 10:2686. doi: 10.1038/s41467-019-10387-7

3. Mcgovern DP, Kugathasan S, Cho JH. Genetics of inflammatory boweldiseases. *Gastroenterology.* (2015) 149:1163–76.e2. doi: 10.1053/j.gastro.2015.08.001

4. Wlodarska M, Kostic AD, Xavier RJ. An integrative view of microbiome-host interactions in inflammatory bowel diseases. *Cell Host Microbe.* (2015) 17:577–91. doi: 10.1016/j.chom.2015.04.008

5. Schwerd T, Bryant RV, Pandey S, et al. NOX1 loss-of-function genetic variants in patients with inflammatory bowel disease. *Mucosal Immunol.* (2018) 11:562–74. doi: 10.1038/mi.2017.74

6. Motta JP, Wallace JL, Buret AG, et al. Gastrointestinal biofilms in health and disease. *Nat Rev Gastroenterol Hepatol.* (2021) 18:314–34. doi: 10.1038/s41575-020-00397-y

7. Parsek MR, Fuqua C. Biofilms2003: emerging themes and challenges in studies of surface-associated microbial life. *J Bacteriol.* (2004) 186:4427–40. doi: 10.1128/JB.186.14.4427-4440.2004

8. Breugelmans T, VanSpaendonk H, DeMan JG, et al. In-depthstudy of transmembranemucins in association with intestinalbarrierdysfunction During the course of T celltransfer and DSS-inducedcolitis. *J Crohns Colitis.* (2020) 14:974–94. doi: 10.1093/ecco-jcc/jjaa015

9. Bantel H, Berg C, Vieth M, et al. Mesalazine inhibits activation of transcription factor NF-kappaB in inflamed mucosa of patients with ulcerative colitis. *Am J Gastroenterol.* (2000) 95:3452–7. doi: 10.1111/j.1572-0241.2000.03360.x

10. Ohkusa T, Kato K, Terao S, et al. Newly developed antibiotic combination therapy for ulcerative colitis: a double-blind placebo-controlled multicenter trial. *Am J Gastroenterol.* (2010) 105:1820–9. doi: 10.1038/ajg.2010.84

11. Panpetch W, Hiengrach P, Nilgate S, et al. Additional Candida albicans administration enhances the severity of dextran sulfate solution induced colitis mouse model through leaky gut-enhanced systemic inflammation and gut-dysbiosis but attenuated by Lactobacillus rhamnosusL34. *Gut Microbes.* (2020) 11:465–80. doi: 10.1080/19490976.2019.1662712

12. Rao K, Higgins PD. Epidemiology, diagnosis, and management of Clostridium difficile infection in patients with inflammatory boweldisease. *Inflammation Bowel Dis.* (2016) 22:1744–54. doi: 10.1097/MIB.0000000000000793

13. Motta JP, Allain T, Green-Harrison LE, et al. Iron sequestration in microbiotabiofilmsas A novelstrategy for treatinginflammatory boweldisease. *Inflammation Bowel Dis.* (2018) 24:1493–502. doi: 10.1093/ibd/izy116

14. Motta JP, Flannigan KL, Agbor TA, et al. Hydrogen sulfide protects from colitis and restores intestinal microbiota biofilm and mucus production. *Inflammation Bowel Dis.* (2015) 21:1006–17. doi: 10.1097/MIB.0000000000000345

15. Zhou H, Weir MD, Antonucci JM, et al. Evaluation of three-dimensional biofilms on antibacterial bonding agents containing novel quaternary ammonium methacrylates. *Int J Oral Sci.* (2014) 6:77–86. doi: 10.1038/ijos.2014.18

16. Cheng L, Weir MD, Zhang K, et al. Antibacterial nanocomposite with calcium phosphate and quaternary ammonium. *J Dent Res.* (2012) 91:460–6. doi: 10.1177/0022034512440579

17. Wu J, Zhou H, Weir MD, et al. Effect of dimethylaminohexadecyl methacrylate mass fraction on fracture toughness and antibacterial properties of CaP nanocomposite. *J Dent.* (2015) 43:1539–46. doi: 10.1016/j.jdent.2015.09.004

18. Wirtz S, Popp V, Kindermann M, et al. Chemically induced mouse models of acute and chronic intestinal inflammation. *Nat Protoc.* (2017) 12:1295–309. doi: 10.1038/nprot.2017.044

19. Lee JG, Lee YR, Lee AR, et al. Role of the global gut microbial community in the development of colitis-associated cancer in a murine model. *BioMed Pharmacother.* (2021) 135:111206. doi: 10.1016/j.biopha.2020.111206

20. Lin JC, Wu JQ, Wang F, et al. QingBai decoction regulates intestinal permeability of dextran sulphate sodium-induced colitis through the modulation of notch and NF-κB signalling. *Cell Prolif.* (2019) 52:e12547. doi: 10.1111/cpr.12547

21. Perey AC, Weishaar IM, Mcgee DW. The effect of ROCK on TNF-α-induced CXCL8 secretion by intestinal epithelial cell lines is mediated through MKK4 and JNK signaling. *CellImmunol.* (2015) 293:80–6. doi: 10.1016/j.cellimm.2014.12.011

22. Zuo L, Kuo WT, Turner JR. Tight junctions as targets and effectors of mucosalimmunehomeostasis. *Cell Mol Gastroenterol Hepatol.* (2020) 10:327–40. doi: 10.1016/j.jcmgh.2020.04.001

23. Nakakura S, Matsui M, Sato A, et al. Pathophysiological significance of the two-pore domain K(+) channel K2P5.1 in splenic CD4(+)CD25(-) T cell subset from a chemically-induced murine inflammatory bowel disease model. *Front Physiol.* (2015) 6:299. doi: 10.3389/fphys.2015.00299

24. Chassaing B, Aitken JD, Malleshappa M, et al. Dextran sulfate sodium (DSS)-induced colitis in mice. *CurrProtocImmunol.* (2014) 104:15–25. doi: 10.1002/0471142735.im1525s104

25. Dahl JU, Gray MJ, Bazopoulou D, et al. The anti-inflammatory drug mesalamine targets bacterial polyphosphate accumulation. *Nat Microbiol.* (2017) 2:16267. doi: 10.1038/nmicrobiol.2016.267

26. Ohkusa T, Nomura T, Terai T, et al. Effectiveness of antibiotic combination therapy in patients with active ulcerative colitis: a randomized, controlled pilot trial with long-term follow-up. *Scand J Gastroenterol.* (2005) 40:1334–42. doi: 10.1080/00365520510023648

27. Wang SL, Wang ZR, Yang CQ. Meta-analysis of broad-spectrum antibiotic therapy in patients with active inflammatory bowel disease. *ExpTherMed.* (2012) 4:1051–6. doi: 10.3892/etm.2012.718

28. Bussières-Marmen S, Vinette V, Gungabeesoon J, et al. Loss of T-cell protein tyrosine phosphatase in the intestinal epithelium promotes local inflammation by increasing colonic stem cell proliferation. *CellMolImmunol.* (2018) 15:367–76. doi: 10.1038/cmi.2016.72

29. Bottery MJ, Passaris I, Dytham C, et al. Spatial organization of expandingbacterialcoloniesisaffected by contact-dependentgrowthinhibition. *Curr Biol.* (2019) 29:3622–3634.e5. doi: 10.1016/j.cub.2019.08.074

30. Qiu X, Zhao X, Cui X, et al. Characterization of fungal and bacterial dysbiosis in young adult Chinese patients with Crohn's disease. *Therap Adv Gastroenterol.* (2020) 13:1756284820971202. doi: 10.1177/1756284820971202

31. Swidsinski A, Weber J, Loening-Baucke V, et al. Spatial organization and composition of the mucosal flora in patients with inflammatory bowel disease. *J Clin Microbiol.* (2005) 43:3380–9. doi: 10.1128/JCM.43.7.3380-3389.2005

32. Ellermann M, Sartor RB. Intestinal bacterial biofilms modulate mucosal immune responses. *J Immunol Sci.* (2018) 2:13–8. doi: 10.29245/2578-3009/2018/2.1122

33. Antón M, Rodríguez-González A, Ballesta A, et al. Alcohol binge disrupts the rat intestinal barrier: the partial protective role of oleoylethanolamide. *Br J Pharmacol.* (2018) 175:4464–79. doi: 10.1111/bph.14501

34. Sun X, Yang Q, Rogers CJ, et al. AMPK improves gut epithelial differentiation and barrier function via regulating Cdx2 expression. *Cell Death Differ.* (2017) 24:819–31. doi: 10.1038/cdd.2017.14

35. Bergström JH, Birchenough GM, Katona G, et al. Gram-positive bacteria are held at a distance in the colon mucus by the lectin-like protein ZG16. *Proc Natl Acad Sci USA.* (2016) 113:13833–8. doi: 10.1073/pnas.1611400113

36. Donaldson GP, Lee SM, Mazmanian SK. Gut biogeography of the bacterial microbiota. *Nat Rev Microbiol.* (2016) 14:20–32. doi: 10.1038/nrmicro3552

37. Ma Y, Yue J, Zhang Y, et al. ACF7 regulates inflammatory colitis and intestinal wound response by orchestrating tight junction dynamics. *Nat Commun.* (2017) 8:15375. doi: 10.1038/ncomms15375

38. Ohkusa T, Koido S. Intestinal microbiota and ulcerative colitis. *J Infect Chemother.* (2015) 21:761–8. doi: 10.1016/j.jiac.2015.07.010

39. Bell A, Brunt J, Crost E, et al. Elucidation of a sialic acid metabolism pathway in mucus-foraging Ruminococcusgnavus unravels mechanisms of bacterial adaptation to the gut. *NatMicrobiol.* (2019) 4:2393–404.

40. Kimyon Ö, Das T, Ibugo AI, et al. Serratia secondarymetaboliteprodigiosininhibits Pseudomonas aeruginosa biofilmdevelopment by producingreactive oxygen species that damagebiologicalmolecules. *FrontMicrobiol.* (2016) 7:972.

41. Hughes G, Webber MA. Novel approaches to the treatment of bacterial biofilm infections. *Br J Pharmacol.* (2017) 174:2237–46. doi: 10.1111/bph.13706

42. Motta JP, Denadai-Souza A, Sagnat D, et al. Active thrombin produced by the intestinal epithelium controls mucosal biofilms. *Nat Commun.* (2019) 10:3224. doi: 10.1038/s41467-019-11140-w

43. Chew SS, Tan LT, Law JW, et al. Targeting gutmicrobialbiofilms-A key to hindercoloncarcinogenesis? *Cancers.* (2020) 12.

44. Dejea CM, Fathi P, Craig JM, et al. Patients with familial adenomatous polyposis harbor colonic biofilms containing tumorigenic bacteria. *Science.* (2018) 359:592–7. doi: 10.1126/science.aah3648

45. Fessler J, Matson V, Gajewski TF. Exploring the emerging role of the microbiome in cancer immunotherapy. *JImmunotherCancer.* (2019) 7:108. doi: 10.1186/s40425-019-0574-4

46. Parian A, Limketkai B, Koh J, et al. Appendectomy does not decrease the risk of future colectomy in UC: results from a large cohort and meta-analysis. *Gut.* (2017) 66:1390–7. doi: 10.1136/gutjnl-2016-311550